Heliyon 8 (2022) e11271

Contents lists available at ScienceDirect

Heliyon

journal homepage: www.cell.com/heliyon

Research article

First-in-human autologous implantation of genetically modified adipocytes expressing LCAT for the treatment of familial LCAT deficiency

Masayuki Aso [a,1], Tokuo T. Yamamoto [a,*], Masayuki Kuroda [b,1], Jun Wada [c], Yoshitaka Kubota [d], Ko Ishikawa [e], Yoshiro Maezawa [e], Naoya Teramoto [e], Ayako Tawada [f], Sakiyo Asada [a], Yasuyuki Aoyagi [a], Mika Kirinashizawa [a], Akinobu Onitake [a], Yuta Matsuura [a], Kunio Yasunaga [a], Shun-ichi Konno [a], Katsuaki Nishino [a], Misato Yamamoto [a], Junko Miyoshi [a], Norihiko Kobayashi [a], Masami Tanio [a], Takayuki Ikeuchi [g], Hidetoshi Igari [h], Nobuyuki Mitsukawa [d], Hideki Hanaoka [g], Koutaro Yokote [e,**], Yasushi Saito [i]

[a] *CellGenTech, Inc., 2600856 Chiba, Japan*
[b] *Center for Advanced Medicine, Chiba University Hospital, 2608677 Chiba, Japan*
[c] *Department of Nephrology, Rheumatology, Endocrinology and Metabolism, Okayama University Graduate School of Medicine, Dentistry and Pharmaceutical Sciences, 7008530 Okayama, Japan*
[d] *Department of Plastic and Reconstructive Surgery, Chiba University, Faculty of Medicine, 2608670 Chiba, Japan*
[e] *Department of Endocrinology, Hematology, and Gerontology, Chiba University, Graduates School of Medicine and Department of Diabetes, Metabolism, and Endocrinology, Chiba University Hospital, 2608670 Chiba, Japan*
[f] *Department of Ophthalmology and Visual Science, Chiba University Graduate School of Medicine, 2608670 Chiba, Japan*
[g] *Chiba University Hospital Clinical Research Center, 2608677 Chiba, Japan*
[h] *Division of Infection Control, Chiba University Hospital, 2608677 Chiba, Japan*
[i] *Chiba University, 2608670 Chiba, Japan*

ARTICLE INFO

Keywords:
Cholesterol homeostasis
Ex vivo gene therapy
Familial LCAT deficiency
HDL
LCAT
Proteinuria
Renal injury

ABSTRACT

Background: Familial lecithin: cholesterol acyltransferase (LCAT) deficiency (FLD) is a severe inherited disease without effective treatment. Patients with FLD develop severe low HDL, corneal opacity, hemolytic anemia, and renal injury.
Objective: We developed genetically modified adipocytes (GMAC) secreting LCAT (LCAT-GMAC) for *ex vivo* gene therapy. GMACs were prepared from the patient's adipocytes to express LCAT by retroviral gene transduction to secrete functional enzymes. This study aimed to evaluate the safety and efficacy of LCAT-GMAC implantation in an FLD patient.
Methods: Proliferative preadipocytes were obtained from a patient using a ceiling culture and retrovirally transduced with LCAT. After obtaining enough cells by expansion culture of the transduced cells, the resulting LCAT-GMACs were implanted into a patient with FLD. To evaluate the safety and efficacy, we analyzed the outcome of the autologous implantation for 24 weeks of observation and subsequent 240 weeks of the follow-up periods.
Results: This first-in-human autologous implantation of LCAT-GMACs was shown to be safe by evaluating adverse events. The LCAT-GMAC implantation increased serum LCAT activity by approximately 50% of the baseline and sustained over three years. Consistent with increased LCAT activity, intermediate-density lipoprotein (IDL) and free cholesterol levels of the small and very small HDL fractions decreased. We found the hemoglobin/haptoglobin complex in the hemolyzed pre-implantation sera of the patient. After one week of the implantation, the hemoglobin/haptoglobin complex almost disappeared. Immediately after the implantation, the patient's proteinuria decreased temporarily to mild levels and gradually increased to the baseline. At 48 weeks after implantation, the patient's proteinuria deteriorated with the development of mild hypertension. By the treatment with antihypertensives, the patient's blood pressure normalized. With the normalization of blood pressure, the proteinuria rapidly decreased to mild proteinuria levels.
Conclusions: LCAT-GMAC implantation in a patient with FLD is shown to be safe and appears to be effective, in part, for treating anemia and proteinuria in FLD.

* Corresponding author.
** Corresponding author.
E-mail addresses: yamamotot@cellgentech.com (T.T. Yamamoto), kyokote@faculty.chiba-u.jp (K. Yokote).
[1] Masayuki Aso and Masayuki Kuroda contributed equally.

https://doi.org/10.1016/j.heliyon.2022.e11271
Received 14 October 2021; Received in revised form 21 February 2022; Accepted 20 October 2022

1. Introduction

Cholesterol esterification catalyzed by lecithin: cholesterol acyltransferase (LCAT) is the most critical step in cholesterol homeostasis [1, 2, 3]. LCAT catalyzes cholesteryl esters (CEs) formation using cholesterol and phosphatidylcholine, producing most plasma CEs. The human LCAT protein is primarily synthesized in the liver, secreted into the blood, and circulates in association with high-density lipoprotein (HDL). LCAT-mediated cholesterol esterification mainly occurs on nascent HDL. In humans, approximately 90% of CEs in plasma are synthesized by LCAT localized on the surface of HDL [4]. The esterified cholesterol migrates to the core of the HDL particle, promoting its maturation. LCAT maintains unesterified cholesterol homeostasis between peripheral cells and HDL particles. Efflux of cholesterol occurs by the transportation of cholesterol between the cellular membrane and the acceptor HDL facilitated by ATP-binding cassette transporter 1. Together with HDL, LCAT plays a critical role in reverse cholesterol transport. The failures of reverse transportation mediated via LCAT, ATP-binding cassette transporter 1, and HDL eventually promote the peripheral cholesterol accumulation in renal disease, and hemolytic anemia in patients with LCAT deficiency [5, 6].

Mutations in the LCAT gene impair the esterification of free cholesterol (FC) to CEs. As a result, reverse cholesterol transportation from the peripheral tissues to the liver is disrupted. The LCAT gene disorder is an autosomal recessive trait, and its prevalence is less than one in a million. Currently, more than 80 mutations have been identified in the LCAT gene [2]. Inherited mutations in the LCAT gene cause two clinically distinct syndromes: familial LCAT deficiency (FLD) and fish-eye disease (FED). Patients with FLD and patients with FED have markedly low HDL-cholesterol (HDL-C) levels and develop corneal opacity. There are no available effective remedies for FLD or FED. FLD is characterized by almost deficient enzyme activity, severely low HDL-C levels, hemolytic anemia, and renal injury. The prognosis of patients with FLD is unfavorable, and the patients eventually develop renal failure.

Enzyme replacement therapy is one of the effective treatment options for FLD [7, 8, 9]. Shamburek et al. conducted a first-in-human clinical study using recombinant human LCAT [10]. A patient with FLD was intravenously administered high doses of recombinant human LCAT over seven months. There were no infusion site reactions or infusion toxicities. Other than favorable changes in renal parameters, no other clinically meaningful shifts in the laboratory or physical examination parameters were observed [10]. LCAT concentration in the patient peaked at the end of the infusion period but then fell close to the baseline value over seven days. The renal function of the patient generally stabilized or improved, and the anemia improved. After infusion, the HDL-C level increased rapidly, peaked near-normal levels in 8–12 h, resulting in rapid sequential disappearance of preβ-HDL and small α-4 HDL and the appearance of normal α-HDL. The patient's 24-hour urinary protein level improved at the end of the treatment phase, and it is estimated that the treatment delayed hemodialysis by eight months. Although recombinant human LCAT therapy was shown to be safe, well-tolerated, and effective, frequent infusion (weekly or biweekly) of a large quantity of the enzyme (a dose of 9.0 mg/kg) is required to maintain its effectiveness [10].

We have been developing an *ex vivo* gene therapy using preadipocytes to treat genetic disorders, including FLD [11, 12, 13, 14, 15] and diabetes [16]. Proliferative preadipocytes are beneficial in *ex vivo* gene therapy. A large quantity of fat can readily be obtained from subcutaneous fat by liposuction, a standard procedure in plastic surgery. Adipocytes are selectively isolated using floating centrifugation after collagenase treatment of the harvested tissues. The cells were then subjected to ceiling culture to obtain highly purified mature adipocytes [17]. Preadipocytes obtained from the ceiling culture are highly proliferative, allowing for high retroviral transduction efficiency of foreign genes and yielding several billions of cells for implantation. Once implanted in the body, the cells undergo final differentiation into adipocytes. The highly

Table 1. Key resources.

Reagent or resource	Source	Identifier
Antibodies		
Anti-CD105-FITC	Ancell	Cat#326-040
Anti-CD13-FITC	Becton Dickinson	Cat#IM0778
Anti-CD146-FITC	Becton Dickinson	Cat#550315
Anti-CD31-FITC	Becton Dickinson	Cat#555445
Anti-CD34-FITC	Beckman Coulter	Cat#IM1870
Anti-CD45-PE	Beckman Coulter	Cat#IM1833
Anti-CD90-PE	Becton Dickinson	Cat#555596
Anti-HLA-ABC-FITC	Becton Dickinson	Cat#555553
Isotype Control IgG1-FITC	Beckman Coulter	Cat#A07795
Isotype Control IgG1-PE	Beckman Coulter	Cat#A07796
Isotype Control IgG2a-PE	BD Pharmingen	Cat#555574
Isotype Control IgG2b-PE	BD Pharmingen	Cat#555743
Isotype Control IgM-FITC	Beckman Coulter	Cat#IM1269
Rabbit Anti-LCAT polyclonal antibodies	Novus biologicals	Cat#NB400-107
Mouse monoclonal anti-human haptoglobin	Abcam	Cat#ab13429
Mouse TrueBlot ULTRA: Anti-Mouse Ig HRP	ROCKLAND	Cat#18-8817
Protein G-HRP conjugate	Millipore	Cat#18-161
Rabbit monoclonal anti-human Anti-LCAT [clone#EPR1384Y]	Abcam	Cat#ab51060
Rabbit monoclonal anti-human hemoglobin beta/ba1	Abcam	Cat#ab214049
Rabbit TrueBlot: Anti-Rabbit IgG HRP	ROCKLAND	Cat#18-8816
TrueBlot Anti-Rabbit Ig IP Beads	ROCKLAND	Cat#00-8800-25
Bacterial and virus strains		
Retroviral vector CGT_hLCATRV	Takara Bio	This study
Biological samples		
Apolipoprotein A1	Athens Research & Technology	Cat#16-16-120101
Beriplast P Combi-Set Tissue adhesion	CSL Behring	N/A
Human plasma HDL	Merck Calbiochem	437641
Human serum	Kohjin bio	Cat#12181201
Chemicals, peptides, and recombinant proteins		
Novo-Protamine Sulfate 100mg for I.V. Inj.	Mochida Pharmaceutical	N/A
CelLytic M, Cell Lysis Reagent	Sigma-Aldrich	Cat#C2978
AdipoRed	Lonza	Cat#PT-7009
DAPI solution	DOJINDO LABORATORIES	Cat#340-07971
Luminata Forte Western HRP Substrate	Merck Millipore	WBLUF0500
OilRedO	MUTO PURE CHEMICALS	Cat#4049-1
[1,2–^{3}H (N)]-cholesterol	American Radiolabeled Chemicals	Cat#ART 0255-1 mCi
[1,2–^{3}H (N)]-cholesterol	Perkin Elmer	Cat#NET139250UC
dimyristoyl phosphatidylcholine (DMPC)	Tokyo Chemical Industry	Cat#D3924
Critical commercial assays		
Bovine albumin ELISA	Bethyl Laboratories	Cat#E11-113
Collagenase Assay Kit-IBL	Immuno-Biological Laboratories	Custom
Gentamicin ELISA	BIOO Scientific	Cat#1027-01A
Retro-X Integration Site Analysis Kit	Clontech	Cat#631467
DNeasy Blood & Tissue Kit	QIAGEN	Cat#69504

(*continued on next page*)

Table 1 (*continued*)

Reagent or resource	Source	Identifier
SYBR Premix Ex Taq Kit	Takara Bio	Cat# RR041A
Experimental models: Cell lines		
Hela	ATCC	Cat#CCL-2
HEK293	ATCC	Cat#CRL-1573
GP + E-86	ATCC	Cat#CRL-9642
GP + envAM-12	ATCC	Cat#CRL-9641
Experimental models: Organisms/strains		
Mouse: NOD.Cg-*Prkdc*^{scid}*Il2rg*^{tm1Wjl}/SzJ	Charles River	Cat#00JO11
Other		
MesenPRO RS^{TM} Medium	Thermo Fisher	Cat#12746012
PGM$^{™}$ Bullet Kit	Lonza	Cat#PT-8002
HyClone SFM4HEK293 Media	HyClone	Cat#SH30521.02
Flexible TLC plates	GE Healthcare Whatman	Dc-Alu Foil Silic Gel 60 F25425
Novex WedgeWell 4–20%, Tris-Glycine	Thermo Fisher	Cat#XP04205BOX
Phenyl Sepharose 6 Fast Flow	Cytiva	Cat#17097310

differentiated adipocytes have a long half-life [18] high secretory ability of cytokines [19, 20], and resistance to transformation [21].

To treat FLD, we performed first-in-human autologous implantation of LCAT-GMAC into a patient with FLD. This first-in-human study aimed to assess the safety, feasibility, and efficacy of LCAT-GMAC implantation as a treatment for FLD.

2. Methods

2.1. Materials

Materials and resources used are shown in Table 1.

2.2. Animals and animal study

Animal study was approved by the Committee on the Use and Care of Animals at Chiba University. The animals were housed in individually ventilated cages (maximum of 4 animals/cage) with 12 h dark, 12 h light conditions. Temperature and relative humidity were maintained at 20–25 °C and 40–70%, respectively. The animals were fed food and water *ad libitum*. All mice were maintained in accordance with the guidelines of Association for Assessment and Accreditation of Laboratory Animal Care International (AAALAC) on the care, welfare, and treatment of laboratory animals. The animal experiments were carried out in Charles River Laboratories, Japan.

2.3. In vivo tumorigenicity test

NSG mice (NOD.Cg-*Prkdc*^{scid}*Il2rg*^{tm1Wjl}/SzJ) were obtained from Charles River Co. and used for tumorigenicity tests. Six weeks old male mice were used for *in vivo* tumorigenicity test.

A portion of the LCAT-GMACs (5×10^6 cells) containing 20 mg/mL fibrinogen was mixed with an equal volume of cells (5×10^6 cells) containing 1.25 U/mL thrombin using a Beriplast p-combi device and injected subcutaneously into the back of an NSG mouse. Similarly, HeLa cells (1×10^5 cells/mouse) were injected as described above as a positive control. Mice injected with a cell suspension solution containing fibrinogen and thrombin without cells were negative controls. The mice were palpated weekly for 24 weeks to observe for nodule formation at the injection site. Tumor size was assessed by external measurement of the length and width in two dimensions using a caliper after tumors reached measurable sizes. The tumor volume was calculated using the following formula: volume = 1/2 × length (mm) × (width [mm])^2. The volume of engraftment was determined according to progressive nodule growth at the injection site. Mice were sacrificed 24 weeks after the injection of cells, except the three mice injected with HeLa cells were sacrificed 18 weeks (one mouse) and 20 weeks (two mice) after the injection due to overgrowth of tumors. Mouse tissues were subjected to histological analysis. Serum samples were analyzed for the secretion of LCAT from the implanted LCAT-GMACs.

2.4. Clinical study details

The primary objective of the clinical study was to evaluate the safety and adverse-event profiles of autologous implantation of LCAT-GMAC derived from a patient with FLD. Due to the considerably low frequency of the occurrence of the disease, only one patient participated in this study. Therefore, statistical precision calculations were not possible. The primary and secondary endpoints were evaluated 24 weeks after implantation and the subsequent follow-up observation. Secondary objectives included the feasibility and efficacy of the GMAC-mediated complementation of functional LCAT for the treatment of FLD.

This clinical study (registered in Japan Registry of Clinical Trials: jRCTa030190230 https://rctportal.niph.go.jp/en/detail?trial_id=jRCTa030190230) was approved by the Ministry of Health, Labour and Welfare of Japan, the Second Certified Special Committee for Regenerative Medicine, Osaka University, and the Institutional Review Board of Chiba University Graduates School of Medicine before patient recruitment. Written informed consent was obtained from the patient, and all individuals involved in this study complied with the World Medical Association Declaration of Helsinki (2008). Blood samples from healthy volunteers were obtained after approval by the institutional ethical review and informed consent. In a complete lack of LCAT activity (null mutation), the patient's immune system will incorrectly identify the LCAT proteins produced by the retrovirus vector as a foreign body and develop a humoral and cellular immune reaction against it. To avoid the development of autoantibodies against LCAT, null mutants of FLD were excluded in this study.

The outline and the schedule of activity of this clinical study are shown in Figure 1 and Table 2, respectively. We evaluated the primary and secondary endpoints 24 weeks after implantation and subsequent follow-up for 216 weeks.

2.5. Preparation of preadipocytes from patients with FLD

All cell manipulations for the generation of LCAT-GMAC from the patient were performed in a Good Manufacturing Practice (GMP)-grade cell processing center. After informed consent was granted by the patient with familial LCAT deficiency (FLD), liposuction was performed on the patient to obtain subcutaneous adipose tissue, which was then weighed and digested with collagenase at 37 °C with gentle agitation for 1 h: 1 g wet-tissue/3 mL of Hank's balanced salt solution containing 2 mg/mL collagenase and 40 μg/mL gentamicin. After collagenase treatment, lipid-loaded adipocytes were floated by centrifugation. The floating adipocyte fraction was filtered through a 500-μm mesh strainer and subjected to ceiling culture in culture flasks filled with Dulbecco's modified Eagle's medium (DMEM)/Ham's nutrient mixture F-12 (DMEM/F-12) supplemented with 20% radiated fetal bovine serum (FBS) [11, 17]. After seven days of ceiling culture, cells that grew on the ceiling surfaces were harvested and seeded into culture flasks for retroviral gene transduction.

2.6. Generation of a retroviral vector

The pDON-AI, Moloney murine leukemia virus vector plasmid (TaKaRa Bio Inc., Shiga, Japan) was used to produce a human LCAT-transduction vector (designated pCGThLCAT) as described [11]. We introduced pCGThLCAT into the ecotropic packaging cell line GP + E86 (ATCC#: CRL-9642) to produce a retrovirus vector carrying human LCAT cDNA. The resulting ecotropic virus vector was then used to infect the amphotropic packaging cell line GP + envAM-12 (ATCC#: CRL-9641).

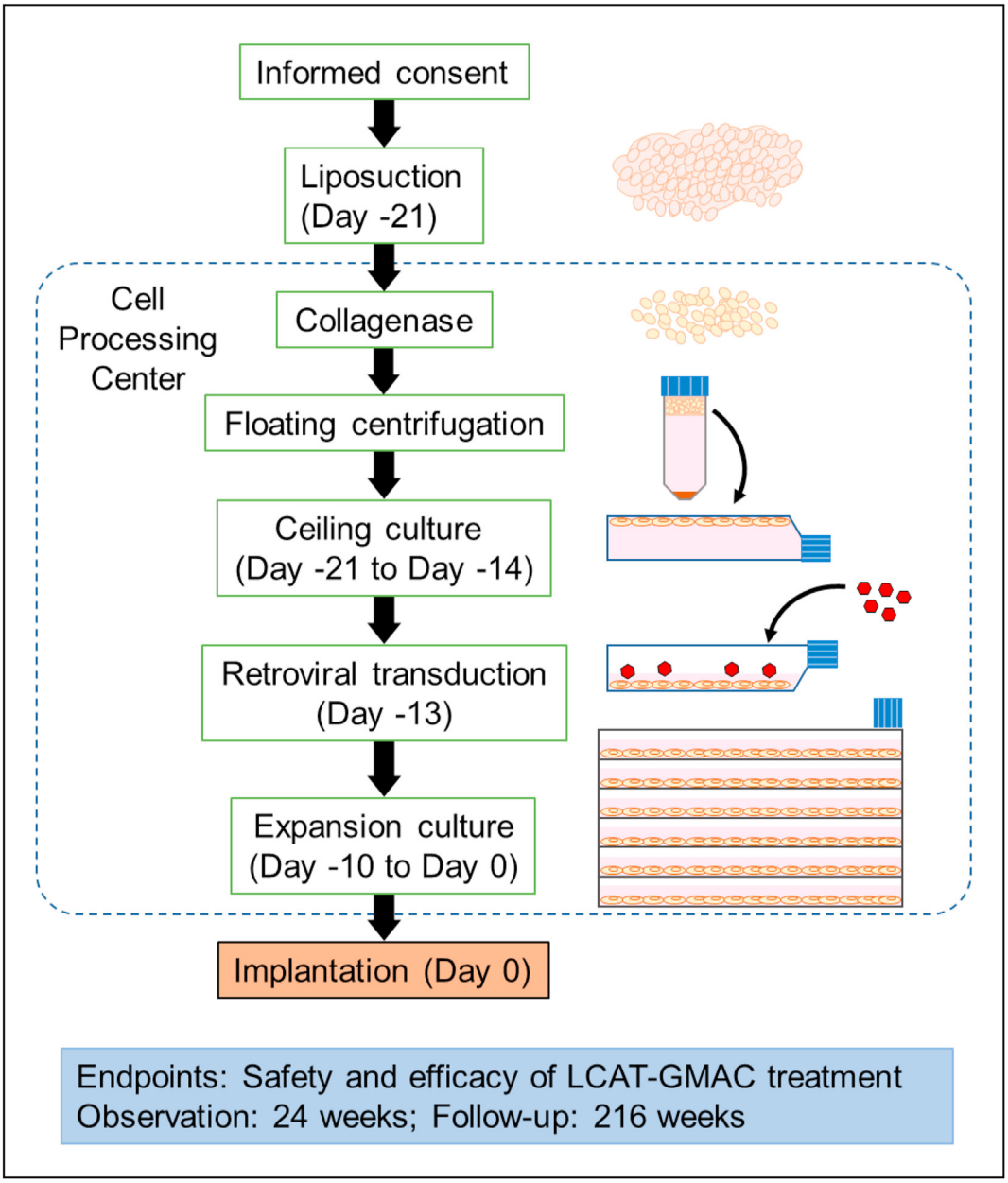

Figure 1. Diagrammatic representation of clinical study on LCAT-GMAC implantation into a patient with FLD.
After obtaining informed consent, the patient underwent liposuction for the preparation of adipocytes. Adipose tissue samples from the patient were digested using collagenase and centrifuged. The lipid-loaded floating cells were then subjected to ceiling culture for one week. After the ceiling culture, highly proliferative pre-adipocytes were obtained. The preadipocytes were transduced with a retrovirus vector carrying LCAT cDNA using the protamine method. After the retroviral transduction, the cells were subjected to expansion culture with MesenPRO RS™ medium containing Growth Supplements in Cell Factory systems at 37 °C in 5% CO_2 incubators for ten days. More than a billion cells were obtained at the end of the expansion culture, and the cells were washed several times and then injected into the patient.

The amphotropic virus vector produced from GP + envAM-12 was designated as CGT_hLCATRV. A master cell bank (MCB) was generated by selecting a cell that produces a high-titer virus vector. The virus vector solution from an MCB was aliquoted and stored at −80 °C until use. TaKaRa Bio Inc. (Shiga, Japan) produced the GMP-grade retroviral vector. In this retrovirus vector system, 5′UTR directs the expression of a foreign gene.

2.7. Retroviral gene transduction for the generation of LCAT-GMACs

After seven days of ceiling culture, the cells were subcultured in DMEM/F-12 containing 20% FBS at 37 °C for 24 h. Viral transduction was performed using protamine sulfate in DMEM/F-12 containing 20% FBS for 24 h at 37 °C. The viral vector concentration used was 2.0×10^9 RNA copies/mL. After the retroviral transduction, the medium was replaced with MesenPRO RS™ containing growth supplements for expansion culture.

2.8. Quantification of transduced gene

Genomic DNA was extracted from cultured cells using the DNeasy Blood & Tissue kit. The integrated vector copy number was quantified using the SYBR Premix Ex Taq kit (TaKaRa Bio Inc.). A known amount of pCGThLCAT DNA was used as a standard. The DNA content in a normal

Table 2. Time schedule and clinical procedures.

Time schedule	Procedures
By day −29	Screening and baseline assessments • Written informed consent • Screening of potential participants according to the inclusion and exclusion criteria • History taking, obtaining documents; Physical exam, blood and urine collection
Day −21	Adipocyte harvesting and baseline assessments • Physical exam, blood and urine collection
Days – 20 and −14	Follow-up assessment of adipocyte harvest sites • Physical exam
Day −1	Follow-up assessment of adipocyte harvest sites and baseline assessments • Inpatient hospital care • Physical exam, blood and urine collection
Day 0	Implantation of LCAT-GMACs: • Inpatient hospital care • Physical exam
Day −1 to day 7	Post-implantation observation: • Inpatient hospital care • Physical exam, blood and urine collection
Week 2 to week 24 (±3 days)	Post-implantation observation: • Inpatient hospital care at 12 weeks • Biweekly observation • Physical examination; blood and urine collection
Week 24 to week 36 (±1 week)	Post-implantation follow-up assessments: • Once every 4 weeks • Inpatient hospital care at 24 weeks • Physical examination; blood and urine collection
Week 48 to week 216 (± 1 week)	Follow-up assessments • Once every 12 weeks • Physical examination; blood and urine collection

Table 3. Quality assessment of LCAT-GMACs derived from the patient.

Test	Specification
Morphology	Conform to proliferating adipocytes with the fibroblast-like shape
Visual inspection	Turbid cell suspension
Cell viability	97.1%
Cell number	1.9×10^9
Average copy number	0.7 copy/cell
LCAT activity	0.6 mU/10^5 cells
Cell surface expression for CD13, CD90, CD105, and CD146	Positive
Cell surface expression for CD31, CD34, and CD45	Negative
Purity: based on the expression of CD31 (−) and CD45 (−) cells	≥90%
Karyotype	Normal
In vitro virus test	Negative
Sterility	Negative
Mycoplasma	Negative
Endotoxin	<0.1 EU/mL
In vivo tumorigenicity	Negative
Clonality determined by LAM-PCR	Negative
Culture medium derived materials	Negative
RCR	Negative

human cell (6 pg/cell) was used for calculating the average integrated copy number. The copy number of transduced genes in an LCAT-GMAC was quantified using a TaqMan Gene Expression Master Mix (Thermo Fisher) and human LCAT-cDNA-specific primers. All real-time PCR analyses were performed using the ABI7500 Real-time PCR system (Thermo Fisher).

2.9. Measurement of LCAT activity

LCAT activity was measured using [1,2–^{3}H (N)]-cholesterol (American Radiolabeled Chemicals Inc., or PerkinElmer Inc., Boston). The reaction mixture contained 22.7 mM Tris-HCl, pH 7.4, 4.5% sucrose, 2.3 mM EDTA, 22.7 mM β-mercaptoethanol, 250 μM cholesterol (specific activity = 2.7 GBq mmol^{-1}), 0.9% bovine serum albumin (BSA), 5 mM dimyristoyl phosphatidylcholine (DMPC), 50 μg/mL of apolipoprotein A1 (ApoA1, Athens Research & Technology), and 100 μL of culture medium or 10 μL of serum in a total volume of 220 μL. [^{3}H]-cholesterol was mixed with non-labeled cholesterol and DMPC in an organic solvent, dried under N_2 gas, and dissolved in 2.25 mL of a buffer containing 50 mM Tris-HCl, pH 7.4, 5 mM EDTA, 10% sucrose, and 275 μg of ApoA1. The DMPC-cholesterol-ApoA1 liposome was prepared by sonication using a digital sonifier model 250 (Branson, Danbury, CT) at an amplitude of 15%. During the sonification procedure, the solution was kept at 37 °C. The sonication was continued until the solution became clear (after about 5 min). The sonicated liposome was centrifuged at 3,000 rpm, and the supernatant (1.8 mL) was mixed with 0.2 mL of 20% BSA and stored at 4 °C until use. After preincubation, the reaction was initiated by adding an enzyme solution and incubated at 37 °C. The reaction was terminated using 1.6 mL of chloroform/methanol (2:1). After adding 100 μL of water and vortexing vigorously, the organic phase was obtained by centrifugation. 50 μL of the organic phase was spotted onto Whatman flexible thin layer chromatography (TLC) plates. TLC plates were developed in a glass chamber using a mixture of hexane, diethyl ether, and acetic acid (146:50:4). After development, the TLC plates were air-dried and stained with iodine. Fractions containing cholesteryl ester on TLC plates were excised. A liquid scintillation counter determined the radioactivities. All assays were performed within the range where the reaction proceeded linearly with time, and the initial rate of reaction was proportional to the amount of enzyme added. The quantity (in nmol) of cholesteryl ester formed per hour was taken as the definition of 1 mU. The purified recombinant LCAT (described below) was used as the standard LCAT. Pooled serum from normal healthy volunteers was used as a reference. The LCAT activity of the reference was 392 ± 34.1 mU/mL (mean ± standard deviation [SD] of 64 independent determinations). The lower reference of LCAT activity was taken to be 5% of the serum diluted with heat-inactivated serum. The lower reference value was 20.9 ± 1.9 (mean ± SD of 64 independent determinations).

2.10. Purification of recombinant LCAT

Recombinant LCAT was purified using a culture medium of 293 cells transduced with LCAT cDNA. The ultrafiltration concentrated (VivaFlow 200 flipflow filtration, MWCO = 50 kDa) enzyme solution (150 mL) from 4 L culture medium (HyClone SFM4HEK293 Media) was used to purify recombinant LCAT. The concentrated enzyme was dialyzed against buffer A (5 mM Na-phosphate buffer, pH7.4 containing 300 mM NaCl) and was applied on a Phenyl-Sepharose column (bed volume: 25 mL) previously equilibrated with buffer A. The column was washed with about 10-column volumes of buffer A, and the enzyme was eluted with water. After the elution, the enzyme solution was added to nine tenth volume of 10 x PBS and concentrated using a centrifugal ultrafiltration device (Amicon Ultra, MWCO = 30 kDa). The purified recombinant LCAT was near homogeneous as judged by SDS-polyacrylamide gel electrophoresis.

2.11. Quantitation of autoantibodies against LCAT

The occurrence of autoantibodies against LCAT was evaluated by enzyme-linked immunosorbent assay (ELISA). Recombinant LCAT was purified from 293 cells expressing LCAT as described and used to capture antibodies against LCAT. Purified recombinant LCAT (67 ng of in 100 μL PBS/well) was incubated overnight to prepare ELISA plates (96-well plate) at 4 °C. The ELISA plates were blocked with 200 μL of

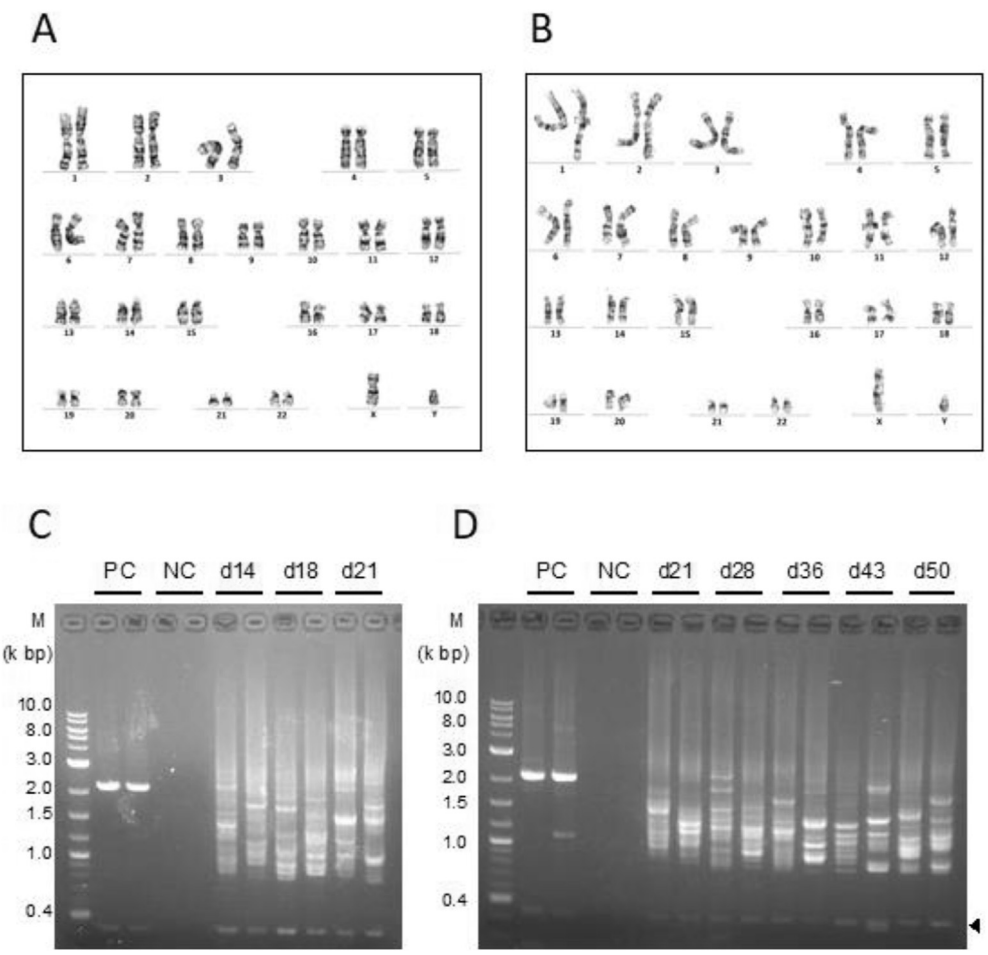

Figure 2. Karyotyping and LAM-PCR analysis.
(A and B) show representative karyotype images of LCAT-GMACs (A) and their parental cells (B), respectively. Metaphase cells (29 days of culture after fat harvest) were subjected to the Giemsa-banding technique, and processed chromosomes were captured and analyzed. LCAT-GMACs were analyzed for clonality using LAM-PCR (C and D). After retroviral transduction (day 7), cells were cultured for seven (labeled d14), eleven (labeled d18), 14 (labeled d21), 21 (labeled d28), 36 (labeled d43), and 43 (labeled d50) days and subjected to LAM-PCR. PC, positive control (human genomic DNA containing 0.1 mg/mL retrovirus vector DNA); NC, negative control with un-transduced parental cells from the patient. The ar shows non-specifically amplified bands with ≈100 bp that appear in all samples. Uncropped original images of C and D are shown as supplementary materials (CS and DS).

Table 4. Adverse events in the patient.

Adverse event	Date of onset	Expression site	Serious adverse event	Treatment	Outcome	Date of the outcome	Causality relationship	Cause of adverse events
Pain	2017/02/02	Fat harvest site	no	Celecoxib + Cefcapene pivoxil hydrochloride hydrate	recovered	2017/02/04	yes	Fat harvest
Pain	2017/02/23	Implantation site	no	Celecoxib + Cefcapene pivoxil hydrochloride hydrate	recovered	2017/02/26	yes	Implantation
Hyper tension	2018/07/10	Blood vessel	no	Telmisartan			no	Unknown
Hyper tension	2018/10/02	Blood vessel	no	Micamlo	controlled		no	Unknown

SuperBlockT20 for 1 h after washing the wells twice with SuperBlockT20 at room temperature. After the blocking, the wells were washed three times with Tris-buffered saline containing 0.05% Tween 20 (TBST). The serum samples were applied for the ELISA after diluting 600 folds with dilution buffer (10% SuperBlockT20 in TBST). Rabbit anti-LCAT antibodies (Abcam, serially diluted to 15, 7.5, 3.75, 1.88, 0.938, 0.469, 0.234, 0.117 ng/mL) were used as standard. The samples were incubated at room temperature for 1.5 h and then washed several times with TBST, followed by incubation with horseradish peroxidase (HRP)-conjugated Protein G at room temperature for 1 h. After several washes with TBST, the HRP reaction was carried out using TMB ELISA substrate according to the manufacture's instruction. Sera obtained from patients with acquired LCAT deficiency [22] were used as positive controls after institutional ethical review and informed consent. This ELISA detected positive signals from the acquired LCAT deficiency patients' sera diluted by 8,000 folds. In contrast, no signals were obtained by pooled serum of healthy persons diluted 600 folds.

2.12. Immunoblot analysis of LCAT protein

Culture medium or serum samples were diluted to a final volume of 500 μL with ice-cold phosphate-buffered saline containing 0.2% Nonidet P-40 (PBS-NP40) and incubated with 1 μL of rabbit anti-LCAT monoclonal antibodies (Abcam) for 18 h at 4 °C with gentle rotation. After the first immunoreaction, 10 μL of TrueBlot anti-Rabbit Ig IP Beads were added and incubated with rotation for 2 h at 4 °C. The IP Beads were pelleted by centrifugation, washed with PBS-NP40, and the immunoprecipitates were eluted by boiling in 10 μL of Laemmli sample buffer. The immunoprecipitates were electrophoresed and subjected to immunoblotting. Purified human LCAT (Roar Biomedical Inc.) or human

Table 5. Serum biochemistry.

Date		Days	Weeks	Total protein (g/dL)	Albumin (g/dL)	Haptoglobin (mg/dL)	Total bilirubin (mg/dL)	Bilirubin (mg/dL)	AST (U/L)	ALT (U/L)	LDH (U/L)	ALP (U/L)	γ-GTP (U/L)	Creatinine (mg/dL)	Uric acid (mg/dL)	BUN (mg/dL)	HbA1c (%)	Cystatin C (mg/L)	eGFRcys (mL/min/1.73 m^2)
2017	1/25	−29		6.9	4.1	34	1.1	0.5	27	25	266	185	10	0.65	5.7	20	ND	ND	ND
	2/2	−21		6.7	4.1	53	0.9	0.4	28	28	233	189	11	0.69	6.1	17	ND	ND	ND
	2/22	−1		6.4	3.9	60	0.9	0.4	26	28	187	167	9	0.69	5.5	19	ND	ND	ND
	2/24	1		6.1	3.7	61	1.4	0.6	43	46	170	154	13	0.70	7.1	22	ND	ND	ND
	2/27	4		6.7	3.9	74	0.9	0.3	37	36	217	143	10	0.65	6.2	14	ND	ND	ND
	3/2	7	1	6.4	3.9	67	0.9	0.3	39	44	202	152	13	0.75	7.2	15	ND	ND	ND
	3/9	14	2	6.9	4.2	74	1	0.5	23	26	171	178	12	0.70	5.4	21	ND	ND	ND
	3/22	27	4	6.8	4.2	54	0.7	0.3	24	24	216	191	13	0.66	5.1	19	ND	ND	ND
	4/6	42	6	6.8	4	114	0.9	0.4	18	22	169	205	10	0.69	5.3	17	ND	ND	ND
	4/20	56	8	6.6	3.9	95	0.6	0.3	16	15	163	237	9	0.69	5.3	19	ND	ND	ND
	5/1	67	10	6.9	4.2	74	0.8	0.4	23	24	168	238	10	0.70	5.0	17	ND	ND	ND
	5/18	84	12	6.7	4.1	74	1.5	0.6	17	18	161	209	9	0.69	5.6	14	ND	ND	ND
	6/16	113	16	6.9	4.2	75	0.8	0.3	20	23	162	239	11	0.60	4.7	18	ND	ND	ND
	7/12	139	20	7.4	4.6	65	1.4	0.8	24	25	178	252	10	0.66	5.0	14	ND	ND	ND
	8/9	167	24	6.4	4.3	52	1.4	0.8	19	20	188	207	9	0.68	4.7	13	ND	ND	ND
	11/1	251	36	6.4	3.8	57	1.2	0.7	22	23	179	213	9	0.70	6.2	13	ND	ND	ND
2018	1/24	335	48	6.5	3.8	64	1	0.5	19	21	186	211	9	0.77	6.1	15	ND	ND	ND
	4/24	425	60	6.5	3.7	104	1	0.5	16	10	171	181	7	0.75	5.5	21	4.1	ND	ND
	7/9	501	72	6.7	4.1	36	1.1	0.6	25	24	186	172	8	0.88	5.4	16	4.2	ND	ND
	10/1	585	84	7.0	4.3	27	1.3	0.6	33	33	216	161	9	0.79	5.4	12	4.2	0.94	88.3
	12/27	672	96	6.8	4.2	79	0.9	0.5	17	16	147	156	11	0.80	6.1	9	4.1	0.89	93.8
2019	3/11	746	108	7.2	4.4	67	0.7	0.4	38	48	181	198	11	0.81	5.3	10	4.1	0.83	100.9
	6/3	830	120	7.1	4.7	64	1.3	0.6	20	20	162	169	8	0.81	4.8	11	3.9	0.99	83.0
	9/2	921	132	7.3	4.5	80	1	0.5	22	23	159	139	10	0.90	6.6	14	4.1	0.94	87.9
	11/27	1007	144	7.1	4.5	72	1.4	0.6	19	17	177	137	8	0.81	6.6	12	4.1	0.95	86.9
2020	2/17	1089	156	6.9	4.5	65	0.8	0.4	41	36	188	188	13	0.78	6.3	19	4.0	0.94	87.5
	5/11	1173	168	6.8	4.3	66	0.9	0.4	27	32	178	156	12	0.82	6.7	18	4.2	0.87	95.3

(*continued on next page*)

Table 5 (*continued*)

Date	Days	Weeks	Total protein (g/dL)	Albumin (g/dL)	Haptoglobin (mg/dL)	Total bilirubin (mg/dL)	Bilirubin (mg/dL)	AST (U/L)	ALT (U/L)	LDH (U/L)	ALP (U/L)	γ-GTP (U/L)	Creatinine (mg/dL)	Uric acid (mg/dL)	BUN (mg/dL)	HbA1c (%)	Cystatin C (mg/L)	eGFRcys (mL/min/1.73 m^2)
8/17	1271	180	7.0	4.6	71	0.9	0.4	26	25	174	103	9	1.02	8.5	25	4.1	0.94	87.5
10/28	1343	192	6.7	4.4	53	1.9	0.9	24	23	169	104	11	0.89	7.1	14	4.1	0.83	100.4
2021 1/18	1425	204	7.3	4.7	55	1.1	0.5	32	24	193	129	12	0.86	6.7	22	4.1	0.84	99.1
4/12	1509	216	6.6	4.4	56	1.1	0.5	25	20	183	36	10	0.87	6.4	18	4.1	0.82	101.3
7/12	1600	228	7.1	4.6	54	1.4	0.7	26	25	177	33	9	0.92	7.9	20	4.2	0.92	89.2
10/6	1686	240	7.3	4.6	64	1.9	0.9	24	22	182	35	11	0.96	8.1	20	4.1	0.97	84.1

AST (Aspartate amino transferase), ALT (Amino alanine transferase), LDH (Lactate dehydrogenase), ALP (Alkaline phosphatase), γ-GTP (gamma glutamyl transpeptidase), BUN (Blood urea nitrogen), CRP (C reactive protein), HbA1c (Hemoglobin A1c), eGFRcys (cystatin C based estimated glomerular filtration rate), ChE (Cholinesterase), ND (not determined).

plasma HDL (Merck Calbiochem) was used as a positive control. Rabbit anti-LCAT polyclonal antibodies (Novus Biologicals) and TrueBlot anti-Rabbit IgG HRP (1:5000) (eBioscience) were used as primary and secondary antibodies, respectively. HRP reactions were performed by incubation with SuperSignal West Femto Maximum Sensitivity Substrate (Thermo Fisher), and chemiluminescence was detected using a Chem-iDoc imaging system (Bio-rad).

2.13. Quality and safety assessment of LCAT-GMACs

LCAT-GMACs were assessed for quality according to the requirements presented in Table 3. Cell viability was evaluated with a NucleoCounter NC-100 (ChemoMetec) using approximately 400 dissociated cells.

The cells were cultured in MesenPRO RS™ medium containing growth supplement for 14 days and subjected to analysis of surface antigen as described previously [11]. Fluorescein isocyanate or phycoerythrin-conjugated antibodies were obtained from BD Farmingen (San Diego, CA), Beckman Coulter (Fullerton, CA), or Ancell (Bayport, MN). One thousand events were acquired and analyzed for each sample on a FACS Calibur apparatus using the Cell Quest™ acquisition software program (Becton Dickinson, Franklin Lakes, NJ).

A soft agar colony formation assay was performed to test for anchorage-independent colony formation. A CytoSelect 96-well Cell Transformation Assay kit was used for this assay according to the manufacturer's instructions (Cell Biolabs, San Diego, CA). Single-cell suspensions of LCAT-GMACs (10^3 cells) were seeded into 96-well plates in triplicates, and HeLa cells (European Collection of Cell Cultures) were used as a positive control.

The karyotyping of LCAT-GMACs and their parental cells (29 days of culture after fat harvest) was performed by LSI Medience Co. (Tokyo, Japan) using a Giemsa-banding technique (GTG-banding technique, Thermo Fisher). Cells were incubated with KaryoMAX Colcemid stock solution (50 ng/mL, Thermo Fisher) at 37 °C for 4 h. Metaphase cells were collected and incubated with 5 mL of hypotonic solution (75 mM potassium chloride), fixed with methanol: acetic acid (3: 1), and subjected to the GTG-banding technique. Processed chromosomes were captured and analyzed.

The clonality of LCAT-GMACs was analyzed with pro-virus integration sites using linear amplification–mediated PCR (LAM-PCR) using the Retro-X Integration Site Analysis Kit according to the manufacturer's instructions.

Replication-competent Retroviruses (RCRs) were tested for in the MCB, working cell bank, vector supernatant, and vector-transduced cells (11 days after retroviral induction) according to the recommendations of the Food and Drug Administration agency (Guidance for Industry: Gene Therapy Clinical Trials – Observing Subjects for Delayed Adverse Events, November 2006, Testing of Retroviral Vector-Based Human Gene Therapy Products for Replication Competent Retrovirus During Product Manufacture and Patient Follow-up. Guidance for Industry, https://www.fda.gov/media/113790/download). A cell-based co-culture RCR test with a known positive control was carried out. The extended S^+/L^- assay was used for cell-based RCR test using the permissive *Mus dunni* cells and subsequent detection of RCR on the PG-4 cell line [23]. PCR-based detection with *psi*-specific primers was also performed for the vector-transduced cells and the patient's serum. These two assays were performed at TaKaRa Bio Inc.

2.14. Lipoprotein analysis using polyacrylamide disc gel electrophoresis and a gel permeation-high performance liquid chromatography (GP-HPLC) system

Lipoprotein profiles were analyzed using polyacrylamide disc gel electrophoresis using the LipoPhor system (JOKOH CO., LTD., Tokyo) as described [24]. An improved HPLC analysis termed GP-HPLC was also performed according to the procedure as described [25, 26, 27, 28]. Polyacrylamide disc gel electrophoresis and GP-HPLC analysis of the

Table 6. LCAT activity, anti-LCAT autoantibodies, and serum lipids.

Date		Days	Weeks	LCAT activity (mU)	LCAT protein (μg/mL)	Anti LCAT Antibody	TG (mg/dL)	TC (mg/dL)	FC (mg/dL)	CE (mg/dL)	CE/TC (%)	HDL –C (mg/dL)	LDL –C (mg/dL)	apoAI (mg/dL)	apoAII (mg/dL)	apoB (mg/dL)	apoCII (mg/dL)	apoCIII (mg/dL)	apoE (mg/dL)
2017	1/25	−29		10.6	6.3	ND	111	80	64	27	34	11	7	50	5.0	50	1.1	2.4	5.1
	2/2	−21		12.5	7.3	ND	138	82	69	22	27	11	7	48	4.5	64	1.7	2.1	5.0
	2/22	−1		12.6	6.4	(−)	132	73	57	27	37	10	7	45	4.9	62	1.4	2.1	4.7
	2/24	1		15.1	6.5	ND	97	70	49	35	51	10	9	40	3.9	59	1.6	2.3	4.9
	2/27	4		15.0	8.2	ND	175	85	61	40	48	10	10	41	5.9	73	2.4	2.4	5.4
	3/2	7	1	16.4	7.1	(−)	158	76	50	44	58	8	9	36	4.5	71	1.8	2.3	5.1
	3/9	14	2	16.2	6.8	(−)	103	75	55	34	45	10	9	49	4.5	66	0.7	1.0	4.4
	3/22	27	4	13.2	6.2	(−)	123	69	56	22	32	10	6	46	4.7	62	0.8	1.2	4.8
	4/6	42	6	13.6	6.5	(−)	104	69	53	27	39	9	6	45	3.7	60	≤0.4	0.7	4.5
	4/20	56	8	14.6	6.6	(−)	139	60	48	20	34	9	5	43	3.9	53	1.6	2.0	3.7
	5/1	67	10	12.0	6.4	(−)	109	61	47	24	39	10	5	50	4.3	52	0.5	1.0	3.9
	5/18	84	12	12.4	6.2	(−)	115	61	46	25	41	10	6	45	5.5	53	1.6	1.5	4.8
	6/16	113	16	13.8	6.6	(−)	100	59	46	22	37	9	4	49	4.0	50	1.0	0.9	4.2
	7/12	139	20	15.0	5.7	(−)	105	61	50	19	30	11	5	50	5.0	54	1.4	0.6	4.3
	8/9	167	24	15.0	5.7	(−)	72	49	39	17	34	10	5	43	3.8	45	1.4	1.1	3.5
	11/1	251	36	15.6	6.0	(−)	95	60	49	19	31	9	5	43	5.0	45	1.3	1.4	4.7
2018	1/24	335	48	17.6	6.3	(−)	109	63	50	22	35	10	6	50	2.5	59	2.5	4.4	5.0
	4/24	425	60	15.1	7.1	(−)	134	82	62	34	41	11	8	48	4.6	71	2.1	2.0	6.4
	7/9	501	72	18.1	7.0	(−)	105	68	53	25	37	10	7	54	4.5	60	0.6	1.4	4.6
	10/1	585	84	16.3	6.1	(−)	92	75	54	35	47	11	10	50	4.0	59	≤0.4	1.0	4.9
	12/27	672	96	17.8	6.6	(−)	87	60	41	32	53	10	8	50	4.3	58	3.0	4.0	4.2
2019	3/11	746	108	20.7	5.5	(−)	99	66	49	29	43	11	8	52	3.9	54	≤0.4	0.9	3.2
	6/3	830	120	17.2	5.6	(−)	81	60	41	32	53	11	10	48	4.2	56	≤0.4	0.3	3.8
	9/2	921	132	18.2	5.8	(−)	97	68	47	35	52	11	8	50	3.9	53	0.5	1.0	4.6
	11/27	1007	144	17.9	5.8	(−)	97	56	43	22	39	10	7	49	4.4	58	0.4	0.7	4.3
2020	2/17	1089	156	19.9	5.4	(−)	97	82	62	34	41	12	12	53	4.3	62	1.1	1.4	4.8
	5/11	1173	168	15.9	6.1	(−)	102	84	67	29	34	11	10	48	3.1	68	0.9	1.3	4.3

(*continued on next page*)

Table 6 (*continued*)

Date	Days	Weeks	LCAT activity (mU)	LCAT protein (μg/mL)	Anti LCAT Antibody	TG (mg/dL)	TC (mg/dL)	FC (mg/dL)	CE (mg/dL)	CE/TC (%)	HDL –C (mg/dL)	LDL –C (mg/dL)	apoAI (mg/dL)	apoAII (mg/dL)	apoB (mg/dL)	apoCII (mg/dL)	apoCIII (mg/dL)	apoE (mg/dL)
8/17	1271	180	18.0	5.6	(–)	116	78	59	32	41	9	8	42	3.7	64	1.4	2.1	3.8
10/28	1343	192	16.5	5.3	(–)	92	81	56	42	52	10	13	43	3.7	64	0.8	1.2	3.8
2021 1/18	1425	204	15.5	5.8	(–)	136	94	74	34	36	11	11	48	3.8	76	1.5	2.6	4.8
4/12	1509	216	18.8	4.5	(–)	103	81	63	30	37	10	8	47	3.4	64	1.4	2.4	3.7
7/12	1600	228	15.5	4.7	(–)	98	76	58	30	40	10	7	47	3.5	58	0.4	1.5	3.4
10/6	1686	240	18.2	7.0	(–)	95	79	61	30	38	11	10	45	3.8	60	1.2	2.1	4.4

TG (Triglyceride), TC (Total Cholesterol), CE (Cholesteryl ester), HDL-C (High density lipoprotein)-cholesterol, LDL-C (Low density lipoprotein)-cholesterol, apoAI (Apolipoprotein AI), apoAII (Apolipoprotein AII), apoB (Apolipoprotein B), apoCII (Apolipoprotein CII), apoCIII (Apolipoprotein CIII), apoE (Apolipoprotein E), ND(not determined), (–): negative. LCAT activity (mU) was expressed as nanomoles of CE formed per mL of serum for 1 h at 37° (E-cho nmol/mL/h).

serum samples were performed at BML Inc. (Tokyo, Japan) and Skylight Biotech Inc (Akita, Japan), respectively.

2.15. Native polyacrylamide gel electrophoresis (PAGE) and immunoblotting

Native-PAGE analysis of serum hemoglobin/haptoglobin complex was performed using Novex Wedgewell 4%–20% Tris-Glycine gels (1.0 mm × 15 wells, Thermo Fisher). Serum samples were mixed with an equal volume of 2X Native Tris-Glycine Sample Buffer (Invitrogen) and electrophoresed using Tris-Borate-EDTA buffer for 3 h with a constant voltage of 100 V at 4 °C. The gels were stained with Coomassie Brilliant Blue G250 or subjected to immunoblotting using the Trans-Blot® Turbo™ Transfer System (Bio-Rad) for protein transfer. Human hemoglobin and haptoglobin were detected with anti-hemoglobin (1 μL/5 mL TBST) and anti-haptoglobin (1 μL/5mL TBST) antibodies, respectively. TrueBlot anti-rabbit IgG HRP (1:5000) (eBioscience) or TrueBlot anti-mouse IgG HRP (1:5000) (eBioscience) were used as secondary antibodies. HRP reactions were performed by incubation with Immobilon Forte Western HRP substrate (Merck Millipore), and chemiluminescence was detected using a ChemiDoc imaging system (Bio-rad).

2.16. Identification of 242 K protein

The 242-kDa protein-containing gel slice was treated with 100 mM dithiothreitol and then alkylated with 100 mM iodoacetamide. After washing, the gel slice was incubated overnight with trypsin at 30 °C. Tryptic peptides derived from the gel-slice were desalted using ZipTip C18 (Millipore) and analyzed with a nano-LC/MS/MS system (Applied Biosystems). Mass data acquisitions were piloted through Mascot software by Japan Proteomics (Sendai, Japan).

2.17. LCAT-GMAC implantation

An LCAT-GMAC suspension (10 mL containing 5×10^8 cells in Ringer solution containing 0.5% human serum albumin and 20 mg/mL fibrinogen) was mixed with an equal volume of cell suspension (5×10^8 cells) in Ringer solution containing 0.5% human serum albumin and thrombin (1.25 U/mL) just before the implantation using a Beriplast P-combi set. For the specific operation procedure, a fat injection cannula was inserted several centimeters cephalad from the inguinal ligament, and the cells were implanted parallel to the inguinal ligament. The injections were performed once on each side.

2.18. Laboratory tests

Unless otherwise stated, all blood biochemistry tests, including serum lipids, lipoproteins, apolipoproteins, hematology tests, and urinalysis, were performed in Hoken Kagaku, Inc. (Yokohama, Japan).

3. Results

3.1. Study design, patient, safety assessment, and LCAT-GMAC implantation

Currently, there is no feasible and effective treatment for FLD. To supplement the defective enzyme in FLD, we designed and performed autologous implantation of LCAT-GMACs in this study.

This clinical study (registered in Japan Registry of Clinical Trials: jRCTa030190230) was approved by the Ministry of Health, Labour and Welfare of Japan. The outline and the schedule of activity of the clinical study are shown in Figure 1 and Table 2, respectively. We evaluated the primary and secondary endpoints 24 weeks after implantation and subsequent follow-up for 216 weeks.

A 34-year-old Japanese man previously diagnosed with FLD based on LCAT gene analysis, markedly low HDL-C and LDL-cholesterol (LDL-C),

Table 7. Lipoprotein analysis by GP-HPLC.

A. Free Cholesterol

			Class	CM (>80 nm)		VLDL (30–80 nm)					LDL (16–30 nm)						HDL (8–16 nm)						
			Sub-Class	–	–	Large VLDL			Medium VLDL	Small VLDL	Large LDL	Medium LDL	Small LDL	Very small LDL			Very large HDL		Large HDL	Medium HDL	Small HDL	Very small HDL	
Date		Days	Fraction Weeks	1	2	3	4	5	6	7	8	9	10	11	12	13	14	15	16	17	18	19	20
2017	1/25	−29		5.04	2.23	3.62	4.94	6.37	4.35	2.82	5.69	4.36	2.80	1.08	2.49	1.73	1.73	1.28	1.15	0.31	0.61	0.42	0.64
	2/2	−21		4.80	2.33	3.70	5.07	5.96	3.96	3.16	6.78	5.33	3.10	1.22	2.39	1.69	1.63	1.26	1.13	0.33	0.69	0.51	0.72
	2/22	−1		2.91	1.51	2.73	3.88	4.87	3.17	3.34	7.28	5.12	3.07	1.20	2.67	1.77	1.67	1.19	1.05	0.37	0.85	0.56	0.74
	2/24	1		2.27	1.28	2.44	3.61	5.02	3.20	2.90	6.48	4.92	2.89	1.17	2.29	1.59	1.51	1.08	0.96	0.25	0.50	0.40	0.66
	2/27	4		2.16	1.28	2.83	4.56	6.32	3.99	3.67	8.64	6.52	4.00	1.67	3.11	2.00	1.84	1.29	1.13	0.39	0.93	0.67	0.78
	3/2	7	1	1.94	1.19	2.41	3.85	5.39	3.33	3.29	8.06	6.17	3.24	1.34	2.38	1.65	1.50	1.08	0.94	0.41	1.01	0.71	0.79
	3/9	14	2	2.58	1.35	2.50	3.61	5.28	3.46	3.14	7.81	6.33	3.59	1.39	2.42	1.70	1.66	1.25	1.15	0.26	0.41	0.32	0.72
	3/22	27	4	2.83	1.37	2.47	3.45	4.63	3.12	2.89	7.79	5.96	3.08	1.25	2.66	1.87	1.80	1.28	1.13	0.32	0.87	0.70	0.73
	4/6	42	6	2.60	1.31	2.36	3.68	5.15	3.18	2.48	6.48	5.31	2.85	1.12	2.18	1.56	1.54	1.13	1.04	0.22	0.34	0.31	0.67
	4/20	56	8	2.47	1.30	2.51	3.70	4.89	3.62	2.65	6.16	4.56	2.85	1.08	2.68	1.82	1.78	1.24	1.07	0.19	0.40	0.28	0.62
	5/1	67	10	1.86	1.03	1.93	2.96	4.41	3.41	2.51	6.30	5.29	3.27	1.28	2.75	1.88	1.85	1.32	1.17	0.23	0.36	0.29	0.65
	5/18	84	12	1.17	0.67	1.39	2.44	3.96	3.25	2.41	5.96	5.10	3.15	1.28	2.63	1.85	1.80	1.36	1.21	0.26	0.35	0.30	0.61
	6/16	113	16	2.29	1.09	2.02	2.94	4.10	3.20	2.40	6.17	4.99	2.52	1.01	2.20	1.58	1.59	1.16	1.08	0.21	0.35	0.33	0.58
	7/12	139	20	1.54	0.84	1.87	3.05	4.60	3.20	2.30	6.71	5.49	3.21	1.37	3.24	2.25	2.21	1.50	1.29	0.27	0.81	0.68	0.69
	8/9	167	24	0.87	0.45	1.02	1.69	2.63	1.95	2.04	6.11	4.83	2.65	1.03	2.53	1.77	1.77	1.27	1.10	0.15	0.35	0.24	0.42
	11/1	251	36	3.09	1.48	2.59	3.67	4.63	3.00	2.19	5.59	4.35	2.27	0.92	2.18	1.57	1.60	1.17	1.09	0.21	0.32	0.22	0.52
2018	1/24	335	48	2.35	1.11	2.12	3.00	3.79	2.57	2.65	6.94	5.26	2.26	0.87	2.21	1.58	1.59	1.15	1.01	0.15	0.38	0.28	0.50
	4/24	425	60	3.42	1.37	2.53	3.92	5.47	3.93	4.29	9.06	6.95	4.40	1.85	3.94	2.61	2.42	1.66	1.43	0.29	0.34	0.53	0.65
	7/9	501	72	2.13	1.06	2.08	3.44	4.79	3.25	3.11	7.40	6.26	3.27	1.36	2.47	1.73	1.65	1.16	1.02	0.17	0.31	0.23	0.61
	10/1	585	84	2.89	1.06	1.59	2.04	3.40	2.86	3.16	8.22	6.66	3.65	1.51	2.80	1.98	1.89	1.34	1.17	0.27	0.57	0.37	0.66
		672	96	1.17	0.64	1.22	1.94	2.76	1.74	3.34	7.65	5.55	2.59	1.01	1.98	1.41	1.37	1.02	0.92	0.15	0.34	0.23	0.42

(*continued on next page*)

Table 7 (*continued*)

A. Free Cholesterol

			Class	CM (>80 nm)		VLDL (30–80 nm)					LDL (16–30 nm)						HDL (8–16 nm)						
			Sub-Class	–	–	Large VLDL			Medium VLDL	Small VLDL	Large LDL	Medium LDL	Small LDL	Very small LDL			Very large HDL		Large HDL	Medium HDL	Small HDL	Very small HDL	
Date		Days	Fraction Weeks	1	2	3	4	5	6	7	8	9	10	11	12	13	14	15	16	17	18	19	20
	12/27																						
2019	3/11	746	108	1.88	0.90	1.68	2.69	4.02	2.97	2.70	6.67	5.57	2.93	1.15	2.12	1.50	1.47	1.08	0.99	0.21	0.41	0.30	0.54
	6/3	830	120	0.64	0.29	0.58	0.92	1.63	1.42	3.02	7.74	6.12	3.10	1.15	2.67	1.90	1.91	1.37	1.21	0.21	0.37	0.22	0.56
	9/2	921	132	1.61	0.77	1.41	2.31	3.72	2.89	3.43	7.68	5.89	3.30	1.36	2.82	1.91	1.84	1.25	1.13	0.20	0.43	0.32	0.85
	11/27	1007	144	1.79	0.86	1.54	2.14	2.65	1.69	2.83	7.49	5.63	2.36	0.82	1.97	1.38	1.39	1.00	0.95	0.18	0.38	0.27	0.60
2020	2/17	1089	156	2.16	1.25	2.70	4.46	7.42	4.32	3.93	8.18	5.91	3.38	1.37	2.57	1.76	1.68	1.15	1.02	0.17	0.34	0.26	0.52
	5/11	1173	168	2.73	1.63	3.33	5.59	8.16	4.56	3.68	9.23	7.28	3.30	1.26	2.25	1.63	1.65	1.24	1.16	0.22	0.38	0.34	0.57
	8/17	1271	180	2.73	1.58	2.98	4.35	6.30	3.83	3.97	8.29	6.59	3.77	1.45	2.48	1.66	1.56	1.13	1.00	0.20	0.30	0.23	0.59
	10/28	1343	192	2.14	1.23	2.54	4.23	6.49	3.52	3.87	9.32	7.01	3.20	1.15	2.14	1.50	1.45	1.07	0.93	0.19	0.29	0.25	0.60
2021	1/18	1425	204	4.85	2.36	4.19	5.18	7.26	4.43	4.54	9.54	6.99	3.69	1.48	2.82	1.85	1.79	1.23	1.08	0.24	0.40	0.33	0.73
	4/12	1509	216	3.93	2.16	4.25	6.18	8.38	4.55	3.60	7.81	5.64	2.82	1.09	2.18	1.45	1.41	0.99	0.86	0.19	0.34	0.32	0.62
	7/12	1600	228	3.18	1.51	2.85	4.03	6.10	3.50	3.80	8.09	6.02	3.03	1.18	2.18	1.50	1.45	1.02	0.90	0.18	0.31	0.26	0.60
	10/6	1686	240	2.90	1.55	3.00	5.14	7.49	4.46	3.74	8.53	6.42	2.89	1.04	2.22	1.54	1.52	1.09	0.99	0.19	0.35	0.25	0.65

B. Phospholipid

			Class	CM (>80 nm)		VLDL (30–80 nm)					LDL (16-30 nm)						HDL (8–16 nm)						
			Sub-Class	–	–	Large VLDL			Medium VLDL	Small VLDL	Large LDL	Medium LDL	Small LDL	Very small LDL			Very large HDL		Large HDL	Medium HDL	Small HDL	Very small HDL	
Date		Days	Fraction Weeks	1	2	3	4	5	6	7	8	9	10	11	12	13	14	15	16	17	18	19	20
2017	1/25	−29		8.62	4.17	7.53	11.07	15.35	11.45	10.04	21.25	16.95	9.36	3.33	8.75	6.47	7.22	5.93	6.95	1.68	8.09	11.16	11.82
	2/2	−21		7.89	3.95	7.27	10.92	14.33	10.51	11.23	24.86	20.14	10.29	3.64	8.25	6.05	6.63	5.46	6.52	1.79	8.78	10.65	9.80
	2/22	−1		4.61	2.58	5.31	8.73	12.33	8.78	12.03	26.08	19.22	9.69	3.72	8.82	6.39	6.65	5.23	6.11	1.59	8.73	9.72	8.59
	2/24	1		4.21	2.39	5.03	8.05	12.25	8.35	10.64	24.03	18.96	9.58	3.58	7.93	5.80	6.09	4.83	5.60	1.32	6.84	8.58	8.86
	2/27	4		4.00	2.61	6.18	11.46	17.05	10.88	13.26	30.58	23.99	12.88	5.25	10.34	7.27	7.28	5.65	6.54	1.87	7.17	9.13	8.59
	3/2	7	1	3.30	2.18	5.21	9.56	14.73	9.00	12.18	29.20	23.77	11.01	4.20	8.10	5.87	5.96	4.72	5.57	1.60	7.39	9.10	7.86

(*continued on next page*)

Table 7 (*continued*)

B. Phospholipid

			Class	CM (>80 nm)		VLDL (30–80 nm)					LDL (16-30 nm)						HDL (8–16 nm)						
			Sub-Class	–	–	Large VLDL			Medium VLDL	Small VLDL	Large LDL	Medium LDL	Small LDL	Very small LDL			Very large HDL		Large HDL	Medium HDL	Small HDL	Very small HDL	
Date		Days	Fraction Weeks	1	2	3	4	5	6	7	8	9	10	11	12	13	14	15	16	17	18	19	20
	3/9	14	2	4.23	2.31	4.74	7.58	12.15	8.30	11.24	27.94	23.37	11.62	4.24	8.10	6.01	6.62	5.33	6.59	1.70	9.13	11.40	9.75
	3/22	27	4	4.72	2.48	4.94	7.56	10.99	7.76	11.54	26.71	21.13	10.84	3.59	8.95	6.28	6.94	5.37	6.31	1.65	7.14	10.68	9.49
	4/6	42	6	4.58	2.57	5.12	8.51	13.18	8.02	10.61	24.29	20.63	10.61	4.05	7.12	5.85	5.82	5.16	5.82	1.61	6.46	10.71	10.55
	4/20	56	8	4.42	2.59	5.41	8.70	12.68	10.49	10.69	22.39	17.67	10.23	3.78	9.50	6.85	7.40	5.72	6.81	1.73	6.80	9.98	11.66
	5/1	67	10	3.34	1.77	3.86	6.52	10.61	8.83	9.36	22.59	18.40	11.30	3.57	9.20	6.48	7.13	5.51	6.46	1.32	7.10	10.61	8.69
	5/18	84	12	2.24	1.33	3.18	6.50	11.05	9.61	9.43	21.61	19.07	11.55	3.72	9.60	6.52	7.30	5.98	6.91	1.79	6.22	9.92	9.23
	6/16	113	16	3.73	2.04	4.06	6.35	9.67	7.99	9.33	21.70	18.59	8.81	3.35	6.76	5.37	5.91	4.79	5.85	1.25	7.35	11.33	10.28
	7/12	139	20	2.48	1.68	3.83	6.73	11.03	7.86	8.78	22.29	19.13	10.49	4.11	9.88	7.44	7.95	6.05	6.71	1.25	6.95	9.71	8.91
	8/9	167	24	1.32	0.97	1.98	3.55	6.26	4.76	8.31	20.84	17.34	8.93	3.41	8.02	6.16	6.82	5.42	6.33	1.29	7.09	9.47	8.12
	11/1	251	36	5.94	3.12	5.78	8.93	11.73	8.30	8.40	20.10	16.58	8.92	3.05	7.52	5.61	6.38	5.44	6.73	1.82	6.39	10.19	11.82
2018	1/24	335	48	4.79	2.58	4.92	7.59	10.09	7.73	10.43	24.55	20.19	9.38	3.03	7.65	5.71	6.43	5.42	6.55	1.72	6.84	11.12	14.21
	4/24	425	60	5.35	2.29	4.73	8.30	12.49	10.01	14.68	29.36	22.57	13.82	4.91	12.45	8.48	8.95	6.64	7.28	2.46	5.17	15.24	14.63
	7/9	501	72	3.50	1.80	3.99	7.22	11.12	8.12	10.95	26.84	22.71	10.38	3.59	7.94	5.94	6.39	4.91	5.57	1.05	7.34	11.60	10.57
	10/1	585	84	4.42	1.58	2.77	3.81	7.05	6.22	10.71	26.20	22.22	10.53	3.58	8.12	6.05	6.55	5.11	5.67	1.22	7.08	10.50	9.69
	12/27	672	96	1.83	1.07	2.35	3.98	5.94	4.03	11.81	25.80	19.53	7.50	2.51	6.01	4.53	5.11	4.14	5.29	1.10	8.32	11.61	11.38
2019	3/11	746	108	3.20	1.62	3.30	5.74	9.40	7.35	9.52	23.20	20.47	9.07	3.07	6.53	4.98	5.44	4.43	5.51	1.97	8.71	11.14	10.36
	6/3	830	120	0.77	0.38	1.11	1.75	3.68	3.18	9.93	25.15	20.67	8.96	3.09	7.67	6.06	6.65	5.38	6.09	1.69	7.23	9.38	9.05
	9/2	921	132	3.00	1.57	3.16	5.45	9.22	8.01	12.22	26.99	22.35	11.02	4.08	9.19	6.76	7.16	5.53	6.45	1.58	8.61	11.30	13.63
	11/27	1007	144	3.06	1.49	3.06	4.54	5.97	3.92	10.26	25.06	19.95	7.16	2.30	5.71	4.48	5.02	4.04	5.25	0.91	8.55	11.52	12.37
2020	2/17	1089	156	3.68	2.05	5.08	8.91	17.01	10.52	12.26	29.81	23.55	10.05	3.70	8.56	6.37	6.81	5.11	5.86	0.79	8.16	11.66	13.03
	5/11	1173	168	4.19	2.58	5.89	10.55	16.16	10.04	10.62	31.82	25.82	10.97	2.70	7.20	5.25	6.05	5.10	5.90	1.40	7.36	10.88	13.07
	8/17	1271	180	4.42	2.70	5.27	8.99	13.61	9.32	14.07	28.12	23.61	12.00	4.08	7.69	5.46	5.81	4.62	5.27	1.32	6.08	9.11	11.80
	10/28	1343	192	3.35	2.07	4.48	7.93	12.86	7.16	12.24	30.94	23.56	8.70	2.92	6.46	4.68	5.56	4.09	5.33	0.47	7.17	9.65	11.35
2021	1/18	1425	204	8.70	4.30	8.37	11.01	16.37	10.58	14.20	33.24	25.46	11.15	4.06	8.74	6.39	6.74	5.32	5.95	1.24	7.92	10.94	13.36
		1509	216	6.76	3.62	8.16	12.13	18.34	10.10	12.57	27.52	21.15	8.59	3.45	6.28	5.17	5.32	4.01	5.30	0.48	7.30	10.51	12.46

(*continued on next page*)

Table 7 (*continued*)

B. Phospholipid

			Class	CM (>80 nm)		VLDL (30–80 nm)					LDL (16-30 nm)						HDL (8–16 nm)						
			Sub-Class	–	–	Large VLDL			Medium VLDL	Small VLDL	Large LDL	Medium LDL	Small LDL	Very small LDL			Very large HDL		Large HDL	Medium HDL	Small HDL	Very small HDL	
			Fraction	1	2	3	4	5	6	7	8	9	10	11	12	13	14	15	16	17	18	19	20
Date		Days	Weeks																				
	4/12																						
	7/12	1600	228	5.62	2.88	5.68	8.28	13.20	8.52	12.60	30.24	22.99	9.62	3.73	7.23	5.57	5.67	4.55	5.42	0.73	7.10	10.19	13.54
	10/6	1686	240	4.11	2.35	5.15	9.50	15.13	9.48	11.59	28.65	22.71	8.26	2.84	6.62	5.31	5.77	4.69	5.65	1.22	7.32	9.30	14.20

C. Triglyceride

			Class	CM (>80 nm)		VLDL (30–80 nm)					LDL (16-30 nm)						HDL (8–16 nm)						
			Sub-Class	–	–	Large VLDL			Medium VLDL	Small VLDL	Large LDL	Medium LDL	Small LDL	Very small LDL			Very large HDL		Large HDL	Medium HDL	Small HDL	Very small HDL	
			Fraction	1	2	3	4	5	6	7	8	9	10	11	12	13	14	15	16	17	18	19	20
Date		Days	Weeks																				
2017	1/25	−29		2.20	2.61	6.85	12.03	12.67	11.60	17.83	27.44	15.27	4.42	1.09	0.54	0.25	0.28	0.13	0.37	0.14	1.42	1.35	1.26
	2/2	−21		2.29	2.40	6.85	14.35	16.44	13.11	20.87	34.49	20.57	6.01	1.55	0.61	0.33	0.30	0.16	0.40	0.21	1.59	1.53	1.33
	2/22	−1		2.06	2.38	7.29	15.15	17.31	12.70	21.49	33.26	18.60	5.44	1.35	0.58	0.29	0.29	0.13	0.42	0.24	1.92	1.64	1.21
	2/24	1		0.99	1.36	4.21	8.33	9.66	8.01	17.65	29.12	17.21	5.08	1.31	0.49	0.26	0.21	0.14	0.24	0.16	0.93	0.99	1.08
	2/27	4		4.31	4.76	13.37	25.50	27.07	14.95	25.85	38.50	20.57	6.00	1.46	0.73	0.35	0.32	0.17	0.45	0.30	2.06	1.63	1.28
	3/2	7	1	3.18	3.44	10.68	22.80	24.74	13.35	23.15	36.53	21.06	6.16	1.58	0.66	0.34	0.31	0.17	0.44	0.36	2.24	1.80	1.21
	3/9	14	2	0.79	0.93	3.16	6.41	7.93	6.77	22.41	36.51	20.44	5.83	1.41	0.54	0.27	0.23	0.15	0.30	0.17	1.04	1.08	1.19
	3/22	27	4	2.17	2.21	5.98	9.64	9.84	7.79	22.29	41.35	20.78	4.06	1.23	0.43	0.32	0.29	0.15	0.38	0.08	2.20	1.98	1.06
	4/6	42	6	0.95	1.18	4.14	8.24	8.81	6.26	20.32	37.28	18.50	3.59	1.08	0.32	0.25	0.21	0.12	0.26	0.03	0.84	1.02	1.06
	4/20	56	8	5.05	3.33	8.29	14.35	15.49	12.26	20.22	33.93	16.72	3.50	1.09	0.44	0.33	0.27	0.20	0.33	0.12	0.93	1.10	1.12
	5/1	67	10	2.58	2.08	5.64	9.75	10.43	8.51	19.27	34.43	17.19	3.53	1.07	0.42	0.31	0.27	0.17	0.34	0.09	1.04	1.19	1.07
	5/18	84	12	1.57	1.98	6.87	15.13	17.85	12.20	18.76	32.74	16.04	3.23	0.97	0.34	0.26	0.21	0.14	0.28	0.08	0.90	0.95	1.05
	6/16	113	16	1.76	1.84	4.72	7.56	7.38	7.51	17.20	30.22	17.50	4.74	1.20	0.47	0.27	0.23	0.15	0.29	0.09	0.89	1.10	1.15
	7/12	139	20	2.14	2.47	5.91	9.23	9.19	6.95	17.97	30.88	16.33	4.33	1.01	0.56	0.28	0.30	0.17	0.40	0.24	1.83	1.57	1.35
	8/9	167	24	0.28	0.32	1.48	3.89	4.19	3.91	15.91	27.46	14.59	3.78	0.84	0.39	0.19	0.19	0.12	0.26	0.10	0.87	0.87	1.09
	11/1	251	36	1.35	1.42	4.92	10.71	9.96	6.67	15.75	27.61	15.58	3.39	1.00	0.29	0.25	0.19	0.16	0.25	0.11	0.59	1.18	1.07
2018		335	48	2.30	1.81	4.75	8.84	8.99	8.00	18.08	33.36	20.51	4.83	1.48	0.33	0.32	0.20	0.19	0.29	0.19	0.89	1.45	1.22

(*continued on next page*)

Table 7 (*continued*)

C. Triglyceride

			Class	CM (>80 nm)		VLDL (30–80 nm)					LDL (16-30 nm)						HDL (8–16 nm)						
			Sub-Class	–	–	Large VLDL			Medium VLDL	Small VLDL	Large LDL	Medium LDL	Small LDL	Very small LDL			Very large HDL		Large HDL	Medium HDL	Small HDL	Very small HDL	
			Fraction	1	2	3	4	5	6	7	8	9	10	11	12	13	14	15	16	17	18	19	20
Date		Days	Weeks																				
	1/24																						
	4/24	425	60	1.74	1.51	4.32	10.76	12.41	13.55	26.05	40.87	24.88	7.66	2.13	0.73	0.46	0.33	0.23	0.33	0.12	0.62	0.97	1.22
	7/9	501	72	0.98	0.98	2.82	6.29	7.29	6.98	21.64	35.41	21.96	5.77	1.85	0.37	0.42	0.25	0.21	0.29	0.09	0.98	1.03	1.16
	10/1	585	84	1.79	1.11	2.02	3.00	4.88	4.55	18.02	36.75	21.49	4.44	1.24	0.33	0.30	0.22	0.14	0.32	0.04	1.34	1.14	1.22
	12/27	672	96	0.58	0.78	2.48	4.40	4.37	3.98	20.31	33.02	17.45	5.63	1.49	0.53	0.31	0.21	0.14	0.27	0.08	1.02	0.93	1.06
2019	3/11	746	108	1.66	1.00	2.33	5.00	7.19	5.61	15.77	31.04	18.31	5.06	1.21	0.60	0.34	0.33	0.23	0.49	0.40	1.57	1.36	1.33
	6/3	830	120	0.31	0.30	0.82	1.94	3.41	2.99	18.10	32.71	19.39	5.86	1.59	0.45	0.31	0.20	0.15	0.29	0.19	0.96	0.81	1.13
	9/2	921	132	0.66	0.72	2.22	5.62	7.30	7.98	21.50	36.67	19.96	4.18	1.43	0.28	0.33	0.21	0.17	0.29	0.13	1.02	1.09	1.11
	11/27	1007	144	2.53	2.22	4.74	6.83	6.57	5.97	18.54	35.39	20.50	4.35	1.45	0.17	0.36	0.21	0.20	0.34	0.13	1.07	1.22	1.22
2020	2/17	1089	156	0.65	0.52	1.67	3.90	5.15	6.88	22.50	35.64	19.19	4.01	1.36	0.33	0.33	0.22	0.16	0.25	0.09	0.84	0.86	1.04
	5/11	1173	168	0.62	0.49	1.18	2.69	4.02	4.45	24.40	41.01	23.53	5.35	1.75	0.26	0.37	0.20	0.18	0.25	0.18	0.80	0.86	1.02
	8/17	1271	180	1.03	0.94	2.51	6.35	9.20	10.12	25.11	41.25	24.32	6.84	1.89	0.51	0.38	0.25	0.18	0.27	0.10	0.76	0.78	1.18
	10/28	1343	192	0.43	0.58	1.89	3.88	4.53	3.54	20.78	35.19	19.68	5.39	1.40	0.60	0.32	0.26	0.18	0.28	0.11	0.72	0.74	1.16
2021	1/18	1425	204	2.90	2.72	5.70	8.71	9.59	9.52	24.59	41.20	24.90	6.80	1.87	0.67	0.43	0.32	0.24	0.34	0.17	0.90	0.96	1.20
	4/12	1509	216	1.14	1.00	2.72	5.80	7.48	7.79	22.92	35.75	20.85	4.99	1.57	0.24	0.37	0.20	0.17	0.24	0.06	0.85	0.91	1.08
	7/12	1600	228	0.89	0.81	1.89	3.14	3.89	5.36	21.57	36.71	21.93	5.39	1.73	0.38	0.39	0.22	0.18	0.24	0.09	0.74	0.93	1.20
	10/6	1686	240	0.78	0.69	2.14	5.20	7.16	5.95	19.35	36.33	20.42	3.65	1.23	0.17	0.32	0.18	0.17	0.22	0.12	0.62	0.98	1.01

D. Cholesteryl Ester

			Class	CM (>80 nm)		VLDL (30–80 nm)					LDL (16–30 nm)						HDL (8–16 nm)						
			Sub-Class	–	–	Large VLDL			Medium VLDL	Small VLDL	Large LDL	Medium LDL	Small LDL	Very small LDL			Very large HDL		Large HDL	Medium HDL	Small HDL	Very small HDL	
			Fraction	1	2	3	4	5	6	7	8	9	10	11	12	13	14	15	16	17	18	19	20
Date		Days	Weeks																				
2017	1/25	−29		−0.17	0.31	0.57	0.69	0.47	0.78	3.25	5.38	2.31	−0.33	−0.33	−0.47	−0.46	−0.34	−0.30	−0.16	−0.10	0.05	0.55	0.33
	2/2	−21		−0.05	−0.05	0.03	0.21	−0.04	0.60	3.00	5.85	3.10	−0.34	−0.46	−0.57	−0.55	−0.35	−0.38	−0.18	−0.12	−0.02	0.47	0.20

(*continued on next page*)

Table 7 (*continued*)

D. Cholesteryl Ester

			Class	CM (>80 nm)		VLDL (30–80 nm)					LDL (16–30 nm)						HDL (8–16 nm)						
			Sub-Class	–	–	Large VLDL			Medium VLDL	Small VLDL	Large LDL	Medium LDL	Small LDL	Very small LDL			Very large HDL		Large HDL	Medium HDL	Small HDL	Very small HDL	
Date		Days	Fraction Weeks	1	2	3	4	5	6	7	8	9	10	11	12	13	14	15	16	17	18	19	20
	2/22	−1		−0.08	0.18	0.40	0.52	0.64	0.98	3.69	6.42	3.54	−0.09	−0.31	−0.75	−0.58	−0.38	−0.29	−0.12	−0.16	−0.16	0.49	0.09
	2/24	1		0.09	0.12	0.45	0.53	0.70	0.84	4.26	8.05	4.72	0.30	−0.27	−0.53	−0.51	−0.34	−0.29	−0.15	−0.11	−0.01	0.34	0.09
	2/27	4		0.11	0.59	1.37	1.47	1.52	0.75	6.12	9.94	4.36	−0.13	−0.46	−0.79	−0.67	−0.48	−0.42	−0.23	−0.18	−0.17	0.33	0.09
	3/2	7	1	0.13	0.32	0.72	1.28	1.35	0.79	5.44	9.74	5.26	0.43	−0.32	−0.54	−0.58	−0.38	−0.34	−0.14	−0.22	−0.21	0.37	0.03
	3/9	14	2	0.06	0.14	0.45	0.30	0.76	0.37	5.43	9.53	4.38	−0.21	−0.43	−0.53	−0.54	−0.38	−0.40	−0.24	−0.08	0.18	0.45	0.08
	3/22	27	4	−0.12	0.17	0.16	0.12	−0.14	0.10	4.00	5.69	2.26	−0.26	−0.29	−0.76	−0.69	−0.60	−0.44	−0.33	−0.19	−0.26	0.16	−0.10
	4/6	42	6	−0.04	0.21	0.51	0.37	−0.10	−0.19	4.47	7.03	2.66	−0.28	−0.24	−0.41	−0.44	−0.43	−0.36	−0.30	−0.08	0.03	0.25	−0.02
	4/20	56	8	−0.02	0.29	0.39	0.13	−0.22	0.03	2.65	3.42	1.27	−0.48	−0.19	−0.74	−0.60	−0.56	−0.39	−0.27	−0.05	−0.06	0.28	0.04
	5/1	67	10	0.30	0.20	0.32	0.30	0.00	−0.09	3.08	4.10	0.95	−0.79	−0.38	−0.78	−0.66	−0.64	−0.49	−0.41	−0.11	0.01	0.23	−0.10
	5/18	84	12	0.13	0.23	0.59	0.95	0.76	0.52	3.94	5.81	1.59	−0.69	−0.45	−0.53	−0.61	−0.57	−0.53	−0.44	−0.16	0.06	0.25	0.01
	6/16	113	16	0.23	0.17	0.04	−0.22	−0.40	0.02	2.16	3.33	1.12	−0.18	−0.25	−0.74	−0.68	−0.64	−0.49	−0.41	−0.10	−0.05	0.10	0.03
	7/12	139	20	0.33	0.37	0.34	0.27	−0.17	−0.40	2.99	4.49	0.95	−0.44	−0.43	−1.10	−0.98	−0.91	−0.65	−0.49	−0.11	−0.29	0.01	0.08
	8/9	167	24	0.18	0.18	0.16	0.01	−0.12	0.02	2.98	4.26	1.24	−0.22	−0.22	−0.75	−0.66	−0.59	−0.44	−0.27	0.01	0.04	0.30	0.32
	11/1	251	36	0.59	−0.02	−0.16	−0.19	−0.71	−0.09	2.56	2.97	1.01	−0.41	−0.32	−0.71	−0.60	−0.58	−0.32	−0.31	0.04	−0.13	0.54	0.39
2018	1/24	335	48	1.47	0.24	0.14	−0.01	−0.19	0.54	3.12	5.04	2.77	0.40	0.10	−0.61	−0.52	−0.50	−0.30	−0.17	0.10	−0.06	0.65	0.49
	4/24	425	60	0.30	0.16	0.21	0.26	−0.37	0.32	3.86	8.30	3.45	−0.48	−0.52	−1.10	−0.88	−0.63	−0.48	−0.35	−0.01	−0.10	0.01	0.25
	7/9	501	72	0.49	0.24	0.16	−0.03	−0.15	0.27	3.78	5.69	3.15	0.59	0.05	−0.64	−0.54	−0.48	−0.30	−0.19	−0.02	0.12	0.30	0.01
	10/1	585	84	0.50	0.12	0.17	−0.01	0.50	−0.18	4.50	9.91	3.14	−0.81	−0.49	−0.77	−0.67	−0.56	−0.46	−0.32	−0.17	0.00	0.42	0.00
	12/27	672	96	0.02	0.08	0.11	0.00	−0.14	0.13	4.93	8.41	2.79	0.48	−0.01	−0.43	−0.42	−0.41	−0.29	−0.18	0.02	0.17	0.39	0.21
2019	3/11	746	108	0.44	0.27	0.24	0.10	−0.01	−0.29	3.30	6.94	2.83	−0.01	−0.24	−0.59	−0.52	−0.49	−0.42	−0.28	−0.04	0.25	0.41	0.15
	6/3	830	120	−0.07	0.07	0.12	0.07	0.43	0.10	4.90	9.33	3.63	0.45	−0.01	−0.62	−0.55	−0.56	−0.40	−0.27	0.00	0.19	0.36	0.11
	9/2	921	132	−0.40	0.06	0.15	0.28	0.16	0.56	4.16	7.74	3.34	−0.72	−0.18	−0.98	−0.63	−0.64	−0.41	−0.39	−0.07	−0.04	0.26	−0.33
	11/27	1007	144	−0.25	0.04	−0.03	−0.12	−0.33	0.19	3.63	6.50	2.84	−0.31	−0.08	−0.78	−0.50	−0.51	−0.35	−0.28	−0.07	0.06	0.40	0.13
2020	2/17	1089	156	−0.10	0.21	0.14	0.11	−0.80	−0.23	6.29	10.92	4.00	−0.34	−0.06	−0.41	−0.27	−0.29	−0.20	−0.18	−0.04	0.16	0.44	0.28
	5/11	1173	168	−0.53	−0.06	−0.38	−0.85	−2.61	−0.84	5.36	7.06	2.82	−0.38	−0.11	−0.80	−0.61	−0.68	−0.51	−0.48	−0.06	0.04	0.16	0.13
		1271	180	0.01	0.22	0.00	−0.01	−0.82	−0.52	5.38	8.68	1.78	−0.68	−0.45	−0.58	−0.55	−0.46	−0.45	−0.31	−0.12	0.06	0.19	0.06

(*continued on next page*)

Table 7 (*continued*)

D. Cholesteryl Ester

			Class	CM (>80 nm)		VLDL (30–80 nm)					LDL (16–30 nm)						HDL (8–16 nm)						
			Sub-Class	–	–	Large VLDL			Medium VLDL	Small VLDL	Large LDL	Medium LDL	Small LDL	Very small LDL			Very large HDL		Large HDL	Medium HDL	Small HDL	Very small HDL	
Date		Days	Fraction Weeks	1	2	3	4	5	6	7	8	9	10	11	12	13	14	15	16	17	18	19	20
	8/17																						
	10/28	1343	192	0.02	0.12	−0.27	−0.46	−1.54	−0.82	6.62	10.08	3.83	0.50	0.00	−0.41	−0.44	−0.39	−0.28	−0.09	−0.02	0.23	0.37	0.23
2021	1/18	1425	204	−0.78	0.21	−0.36	−0.48	−0.96	−0.49	5.21	8.99	2.94	−0.39	−0.36	−0.86	−0.61	−0.60	−0.36	−0.25	−0.12	0.04	0.27	0.04
	4/12	1509	216	0.30	0.44	−0.37	−0.74	−1.60	−0.67	4.46	6.43	3.03	0.08	−0.05	−0.72	−0.45	−0.42	−0.27	−0.15	−0.08	0.05	0.25	0.13
	7/12	1600	228	−0.40	0.20	−0.27	−0.39	−1.09	−0.37	5.22	8.47	2.00	−0.30	−0.10	−0.45	−0.35	−0.40	−0.30	−0.22	−0.08	0.10	0.32	0.32
	10/6	1686	240	0.47	−0.12	−0.19	−0.57	−1.60	−0.98	4.73	9.13	4.08	−0.30	−0.08	−0.77	−0.49	−0.49	−0.29	−0.25	0.00	−0.08	0.59	0.10

Free cholesterol (A), phospholipid (B), triglyceride (D), cholesteryl ester levels in 20 fractions separated by GP-HPLC are shown. Chylomicron (CM), very low-density lipoprotein (VLDL), low-density lipoprotein (LDL), and high-density lipoprotein (HDL) fractions are indicated according to Okazaki and Yamashita [26, 28]. CE concentration was calculated according to Okazaki and Yamashita [26].

Table 8. Hematology tests.

Date		Days	Weeks	Hemolysis	WBC (10^3/μL)	RBC (10^3/μL)	Hb (g/dL)	Ht (%)	MCV (fL)	MCH (pg)	MCHC (%)	PLT (10^3/μL)	Neutrophils (%)	Lymphocyte (%)	Monocyte (%)	Eosinophils (%)	Basophils (%)	Reticulocyte count (per mille)
2017	1/25	−29		(1+)	4.1	3.84	12.0	36.7	95.6	31.3	32.7	194	56.6	36.0	3.7	1.7	2.0	ND
	2/2	−21		(1+)	4.0	3.79	11.9	36.5	96.3	31.4	32.6	177	56.0	35.9	4.5	2.3	1.3	ND
	2/22	−1		(−)	3.3	3.68	11.3	34.5	93.8	30.7	32.8	192	53.3	38.3	5.1	2.7	0.6	ND
	2/24	1		(−)	3.4	3.50	10.6	33.0	94.3	30.3	32.1	162	70.5	21.3	4.7	2.3	1.2	ND
	2/27	4		(1+)	3.2	3.55	11.1	33.9	95.5	31.3	32.7	179	54.0	39.4	3.5	2.2	0.9	ND
	3/2	7	1	(1+)	3.8	3.58	10.8	33.7	94.1	30.2	32.0	176	55.3	37.8	2.9	2.4	1.6	ND
	3/9	14	2	(−)	4.2	3.56	11.0	34.2	96.1	30.9	32.2	171	63.0	30.3	4.3	1.2	1.2	ND
	3/22	27	4	(1+)	4.2	3.68	11.2	34.6	94.0	30.4	32.4	166	58.1	35.5	3.8	1.7	0.9	ND
	4/6	42	6	(−)	5.5	3.66	11.5	35.1	95.9	31.4	32.8	218	75.1	19.9	3.4	1.1	0.5	ND
	4/20	56	8	(−)	4.6	3.72	11.3	35.1	94.4	30.4	32.2	200	66.2	28.1	2.9	2.4	0.4	ND
	5/1	67	10	(−)	5.2	3.75	11.4	34.2	91.2	30.4	33.3	161	66.5	27.5	3.3	2.1	0.6	ND
	5/18	84	12	(−)	3.3	3.77	11.5	34.1	90.5	30.5	33.7	151	50.8	41.4	3.6	3.3	0.9	ND
	6/16	113	16	(−)	5.0	3.75	11.5	34.6	92.3	30.7	33.2	181	70.6	25.6	2.4	0.8	0.6	ND
	7/12	139	20	(−)	4.1	3.68	11.5	34.3	93.2	31.3	33.5	162	59.1	34.5	3.4	2.0	1.0	ND
	8/9	167	24	(−)	3.3	3.55	10.5	32.5	91.5	29.6	32.3	142	61.3	30.8	4.6	2.4	0.9	ND
	11/1	251	36	(−)	4.7	3.59	11.0	33.6	93.6	30.6	32.7	157	63.5	29.7	4.9	1.3	0.6	ND
2018	1/24	335	48	(−)	4.6	3.71	11.5	34.1	91.9	31.0	33.7	175	65.2	28.7	4.1	1.1	0.9	26
	4/24	425	60	(−)	4.4	3.44	10.5	31.8	92.4	30.5	33.0	181	64.0	29.9	4.5	0.9	0.7	21
	7/9	501	72	(−)	3.6	3.45	10.8	31.3	90.7	31.3	34.5	140	62.2	34.0	2.2	0.8	0.8	23
	10/1	585	84	(−)	5.5	3.53	11.2	33.6	95.2	31.7	33.3	170	61.1	32.4	3.4	2.2	0.9	18
	12/27	672	96	(−)	4.6	3.27	10.3	31.1	95.1	31.5	33.1	187	66.1	29.2	2.9	0.9	0.9	16
2019	3/11	746	108	(−)	5.1	3.29	10.5	33.3	101.2	31.9	31.5	184	67.3	27.8	3.7	0.8	0.4	23
	6/3	830	120	(−)	3.9	3.30	10.6	32.0	97.0	32.1	33.1	180	59.4	35.5	3.3	1.3	0.5	17
	9/2	921	132	(−)	3.8	3.02	10.0	30.3	100.3	33.1	33.0	164	58.6	36.6	2.9	1.1	0.8	17
	11/27	1007	144	(−)	5.1	3.28	10.8	32.9	100.3	32.9	32.8	165	69.5	25.3	3.8	0.8	0.6	19
2020	2/17	1089	156	(−)	4.6	3.20	10.0	31.8	99.4	31.3	31.4	163	55.3	37.6	4.3	1.7	1.1	17
	5/11	1173	168	(−)	3.9	3.16	10.1	31.1	98.4	32.0	32.5	159	54.3	38.8	3.3	2.3	1.3	27
		1271	180	(−)	5.5	2.96	9.5	30.8	104.1	32.1	30.8	152	56.7	37.5	3.4	1.3	1.1	16

(*continued on next page*)

Table 8 (*continued*)

Date	Days	Weeks	Hemolysis	WBC (10^3/μL)	RBC (10^3/μL)	Hb (g/dL)	Ht (%)	MCV (fL)	MCH (pg)	MCHC (%)	PLT (10^3/μL)	Neutrophils (%)	Lymphocyte (%)	Monocyte (%)	Eosinophils (%)	Basophils (%)	Reticulocyte count (per mille)
8/17																	
10/28	1343	192	(−)	4.4	2.96	9.5	29.0	98.0	32.1	32.8	143	55.6	38.7	3.2	1.4	1.1	18
2021 1/18	1425	204	(−)	5.8	3.66	11.3	35.8	97.8	30.9	31.6	167	63.4	30.9	4.0	1.2	0.5	15
4/12	1509	216	(−)	5.2	3.11	10.0	30.7	98.7	32.2	32.6	161	55.0	39.8	3.6	1.0	0.6	17
7/12	1600	228	(−)	5.0	3.05	9.7	30.2	99.0	31.8	31.8	123	54.8	38.8	3.8	1.4	1.2	21
10/6	1686	240	(−)	5.2	3.24	10.1	30.3	93.5	31.2	31.2	151	59.1	34.6	4.2	1.3	0.8	17

WBC (White blood cell), RBC (Red blood cell), Hb (Hemoglobin), Ht (Hematocrit), MCV (Mean corpuscular volume), MCH (Mean corpuscular hemoglobin), MCHC (Mean corpuscular hemoglobin concentration), PLT (Platelets), RDW (Red cell distribution width), ND(not determined).
(1+) of Hemolysis: Serum Hb level is 26 mg/dL to 99 mg/dL, (−) of Hemolysis: Serum Hb level is 25 mg/dL or less.

bilateral corneal opacity, and modest proteinuria willingly participated in this study. Nucleotide sequence analysis of the LCAT gene revealed that he is homozygous to a missense mutation (c. 278C > T [p. P69L]) in exon 2 of the LCAT gene [29]. Electron microscopic analysis of the renal biopsy specimen revealed lipid deposits with a vacuolar lucent appearance in the glomerular basement membrane [29]. Before participating in the clinical study, the patient rapidly developed proteinuria, the main reason for deciding to receive LCAT-GMAC implantation. Baseline laboratory parameters included the following: blood urea nitrogen (BUN) level = 20 mg/dL, serum creatinine level = 0.65 mg/dL, 24-hour urine protein level = 1,012 mg, hemoglobin level = 12 g/dL, hematocrit = 36.7%, total cholesterol (TC) level = 80 mg/dL, LDL-C level = 7 mg/dL, HDL-C level = 11 mg/dL, and triglyceride level = 111 mg/dL. A comprehensive list of the patient's clinical parameters is shown in Tables 5, 6, 7, 8, 9, 10, and 11.

In February 2017, the first-in-human implantation of LCAT-GMACs into a patient with FLD was performed in Chiba University Hospital. In this first-in-human study, we evaluated the safety and efficacy of autologous implantation of LCAT-GMACs as a treatment for FLD.

LCAT-GMAC was generated from preadipocytes from the patient subcutaneous adipose tissue via retroviral transduction of LCAT cDNA (diagramed in Figure 1). After treatment of the adipose tissue with collagenase, lipid-loaded cells were floated by centrifugation. The floating adipocyte fraction was subjected to ceiling culture for a week and transduced with a retrovirus vector encoding human LCAT cDNA. The resulting LCAT-GMACs were expanded for subsequent large-scale culture. The average copy number of LCAT-GMACs determined by quantitively PCR was 0.7 copy/cell (Table 3). Karyotyping (Figure 2A and 2B), soft agar colony formation assay and clonality analysis as determined by linear-amplification mediated PCR (LAM-PCR) were carried out for safety measures (Figure 2C and 2D). Quality assessment of the LCAT-GMACs was also performed, including flow cytometry for cell surface antigens (Table 3). After expansion culture for ten days, LCAT-GMACs (10^9 cells) were mixed with fibrinogen and thrombin and injected subcutaneously into both sides of the inguinal adipose tissues (see methods, 2.16).

No severe adverse events associated with implantation were observed, including implantation site reaction or implantation toxicity (Table 4). There were no clinically essential deteriorations in laboratory examination parameters related to hepatic and renal functions during this study (Table 5). Retrovirus-mediated gene transduction has a potential risk of generation of replication-competent retroviruses (RCRs) [30, 31]. Furthermore, insertional mutagenesis mediated by retroviruses may be a risk factor for tumors. Polymerase chain reaction (PCR) analysis of the patient's peripheral blood revealed no evidence of RCRs during the observation period of 24 weeks and over a follow-up period of three years (Figure 3).

3.2. Tumorigenicity monitoring and terminal differentiation of implanted cells into NSG mice

A portion of the LCAT-GMACs derived from the patient were implanted into NSG (NOD. Cg-*Prkdc*^{scid}*Il2rg*^{tm1Wjl}/SzJ) mice [32] to monitor the tumorigenesis. LCAT-GMACs (10^7 cells/mouse) were mixed with fibrin glue [11] and subcutaneously injected into mice. HeLa cells (10^5 cells/mouse) were used as a positive-control reference in the tumorigenicity test. As shown in Figure 4A, HeLa cells developed a palpable mass by eight weeks after implantation. In contrast, the graft cell volumes were unchanged in mice implanted with LCAT-GMACs for 24 weeks after implantation.

Histological analysis revealed that mice injected with Hela cells showed robust tumor development (Figure 4B, the left panel). In contrast, no sign of tumor development in mice implanted with fibrin glue only (Figure 4B, the middle panel) or LCAT-GMACs derived from the patient (Figure 4B, the right panel). In LCAT-GMAC implanted mice, the implanted cells underwent terminal differentiation into mature

Table 9. Urinalysis (spot urine).

Date		Days	Weeks	Occult blood reaction	Urobilinogen	Urine sediment										
						RBC	WBC	Squamous epithelium	Urate	Bacteria	Renal Tubular epithelial cells	Hyaline casts	Granular casts	Mucus thread	Uric acid crystal	Epithelial cast
2017	1/25	−29		(2+)	(±)	(1–4)	(1–4)	<1	(1+)	(−)	(−)	(−)	(−)	(−)	(−)	(−)
	2/2	−21		(1+)	(±)	(5–9)	(1–4)	<1	(−)	(−)	(−)	(−)	(−)	(−)	(−)	(−)
	2/22	−1		(2+)	(±)	(5–9)	(1–4)	<1	(1+)	(1+)	(−)	(−)	(−)	(−)	(−)	(−)
	2/24	1		(1+)	(±)	(1–4)	<1	<1	(3+)	(−)	(−)	(−)	(−)	(−)	(−)	(−)
	2/27	4		(1+)	(±)	(5–9)	(1–4)	<1	(−)	(−)	(−)	(−)	(−)	(−)	(−)	(−)
	3/2	7	1	(2+)	(±)	(5–9)	(1–4)	<1	(3+)	(2+)	(−)	(−)	(−)	(−)	(−)	(−)
	3/9	14	2	(2+)	(±)	(5–9)	(5–9)	<1	(2+)	(−)	(−)	(−)	(−)	(−)	(−)	(−)
	3/22	27	4	(2+)	(±)	(1–4)	<1	<1	(3+)	(−)	(−)	(−)	(−)	(−)	(−)	(−)
	4/6	42	6	(2+)	(±)	(10–19)	(1–4)	<1	(−)	(−)	(−)	(−)	(−)	(−)	(−)	(−)
	4/20	56	8	(2+)	(±)	(10–19)	(1–4)	<1	(−)	(1+)	(−)	(−)	(−)	(−)	(−)	(−)
	5/1	67	10	(2+)	(±)	20–29	(5–9)	<1	(−)	(1+)	(−)	(−)	(−)	(−)	(−)	(−)
	5/18	84	12	(2+)	(±)	(1–4)	<1	<1	(−)	(−)	(1–4)	(30–49)	(−)	(+)	(−)	(1–4)
	6/16	113	16	(2+)	(±)	(20–29)	<1	<1	(−)	(−)	(−)	(−)	(−)	(+)	(−)	(−)
	7/12	139	20	(2+)	(±)	(1–4)	(1–4)	<1	(−)	(−)	(−)	(−)	(−)	(+)	(−)	(−)
	8/9	167	24	(3+)	(±)	(10–19)	<1	<1	(−)	(−)	(1–4)	(10–19)	(1–4)	(+)	(−)	(1–4)
	11/1	251	36	(3+)	(±)	<1	<1	<1	(2+)	(−)	(−)	(−)	(−)	(+)	(−)	(−)
2018	1/24	335	48	(3+)	(±)	(1–4)	<1	<1	(3+)	(−)	(−)	(−)	(−)	(+)	(−)	(−)
	4/24	425	60	(3+)	(±)	(10–19)	(1–4)	<1	(1+)	(−)	(−)	(−)	(−)	(+)	(−)	(−)
	7/9	501	72	(2+)	(±)	(5–9)	(1–4)	<1	(−)	(−)	(−)	(−)	(−)	(+)	(−)	(−)
	10/1	585	84	(3+)	(±)	(10–19)	(1–4)	<1	(−)	(−)	(−)	(−)	(−)	(−)	(−)	(−)
	12/27	672	96	(1+)	(±)	(1–4)	(1–4)	(5–9)	(−)	(−)	(−)	(−)	(−)	(+)	(−)	(−)
2019	3/11	746	108	(1+)	(±)	(1–4)	<1	<1	(−)	(−)	(−)	(−)	(−)	(−)	(−)	(−)
	6/3	830	120	(1+)	(±)	(5–9)	(1–4)	<1	(−)	(−)	(−)	(−)	(−)	(−)	(−)	(−)
	9/2	921	132	(1+)	(±)	(1–4)	(1–4)	<1	(−)	(−)	(−)	(−)	(−)	(−)	(−)	(−)
	11/27	1007	144	(2+)	(±)	(5–9)	<1	<1	(2+)	(−)	<1	(1–4)	(−)	(−)	(1+)	(−)
2020	2/17	1089	156	(1+)	(±)	(5–9)	<1	<1	(−)	(−)	(−)	(−)	(−)	(−)	(−)	(−)
	5/11	1173	168	(1+)	(±)	(1–4)	<1	<1	(−)	(−)	(−)	(1–4)	(−)	(−)	(−)	(−)
	8/17	1271	180	(−)	(±)	(1–4)	<1	<1	(−)	(−)	(−)	(−)	(−)	(−)	(1+)	(−)
	10/28	1343	192	(±)	(±)	<1	(1–4)	<1	(2+)	(−)	(−)	(−)	(−)	(−)	(−)	(−)
2021	1/18	1425	204	(2+)	(±)	(5–9)	(1–4)	<1	(−)	(−)	(−)	(−)	(−)	(−)	(−)	(−)
	4/12	1509	216	(2+)	(±)	(5–9)	(1–4)	<1	(−)	(−)	(−)	(−)	(−)	(−)	(−)	(−)
	7/12	1600	228	(±)	(±)	(1–4)	<1	<1	(−)	(−)	(−)	(−)	(−)	(−)	(1+)	(−)
	10/6	1686	240	(1+)	(±)	(1–4)	(1–4)	<1	(−)	(1+)	(−)	(5–9)	(−)	(−)	(−)	(−)

RBC (red blood cell), WBC (white blood cell), UUN (urine urea nitrogen), β2-MG (beta2 microglobulin), ND (not determined).
Occult blood reaction, Urobilinogen, Protein, Glucose, Ketones, Specific gravity of urine, pH, Bilirubin and Nitrate of spot urine were determined using Eiken Uro-paper alpha III (Eiken Chemical Co., Ltd.).
Urine sediment was analyzed by Hoken Kagaku, Inc. (−) and (+) denote negative and positive respectively. (1+), (2+) and (3+) of Calcium oxalate, Urate and Uric acid crystal designate 1–4, 5–9 and 10 or more crystals/high power field respectively. (1+) of Bacteria denotes that bacteria are found in all fields. (2+) of Bacteria denotes that many bacteria are found in all fields.

Table 10. Urinalysis (24-hour urine collection).

Date		Days	Weeks	Protein (mg/day)	Creatinine (mg/dL)	Creatinine clearance (L/day)	Sodium (g/day)	UUN (g/day)	β2-MG (μg/day)
2017	1/25	−29		1012	169.3	ND	ND	ND	ND
	2/2	−21		712	152.5	ND	ND	ND	ND
	2/22	−1		652	133.6	ND	ND	ND	ND
	2/24	1		ND	ND	ND	ND	ND	ND
	2/27	4		ND	ND	ND	ND	ND	ND
	3/2	7	1	390	168.3	ND	ND	ND	ND
	3/9	14	2	ND	ND	ND	ND	ND	ND
	3/22	27	4	650	277.3	ND	ND	ND	ND
	4/6	42	6	ND	ND	ND	ND	ND	ND
	4/20	56	8	ND	ND	ND	ND	ND	ND
	5/1	67	10	ND	ND	ND	ND	ND	ND
	5/18	84	12	1040	125.5	ND	ND	ND	ND
	6/16	113	16	ND	ND	ND	ND	ND	ND
	7/12	139	20	ND	ND	ND	ND	ND	ND
	8/9	167	24	1287	181.2	ND	ND	ND	ND
	11/1	251	36	833	200.3	ND	ND	ND	ND
2018	1/24	335	48	1890	242.8	ND	ND	ND	ND
	4/24	425	60	2097	137.2	161	(−)	(−)	ND
	7/9	501	72	1530	120.0	144	6	5.2	182
	10/1	585	84	1698	98.2	180	8	5.2	263
	12/27	672	96	375	152.8	158	2	3.8	84
2019	3/11	746	108	295	82.0	174	4	4.1	<51
	6/3	830	120	442	57.3	148	4	4.9	<101
	9/2	921	132	177	138.1	170	5	7.4	103
	11/27	1007	144	238	193.0	137	2	4.2	94
2020	2/17	1089	156	515	114.6	160	5	8.2	90
	5/11	1173	168	316	132.3	203	9	11.6	96
	8/17	1271	180	121	111.7	128	5	8.0	69
	10/28	1343	192	143	199.1	163	3	6.7	110
2021	1/18	1425	204	303	91.3	112	4	6.6	81
	4/12	1509	216	310	120.3	161	6	8.1	70
	7/12	1600	228	126	123.8	134	5	7.5	50
	10/6	1686	240	135	201.9	140	3	7.4	62

adipocytes (Figure 4B, the right panel), which are believed to be resistant to tumor development [21]. In addition, periodical MRI scans showed no sign of occurrence of tumors in the patient.

Immunoprecipitation (IP) Western blot analysis of sera derived from the LCAT-GMAC implanted mice showed noticeable LCAT proteins after 24 weeks of implantation, suggesting long-term secretion of human LCAT from the implanted cells (Figure 4C).

3.3. LCAT activity and autoantibodies

Serum levels of LCAT activity pre- and post-implantation are shown in Figure 5A and Table 6. LCAT activity in the patient increased within 24 h after implantation (approximately 30% induction of the pre-implantation mean values: basal level), peaked one week after implantation, and lasted for two weeks. Thereafter, LCAT activity started to decline rapidly, and it gradually fell to the pre-implantation level by post-implantation week 10. It then slowly recovered and almost plateaued 48 weeks after implantation. The mean value at 48 to 240 post-implantation weeks was about 150% of the pre-implantation value (Figure 5A and Tab2le 6). Although LCAT-GMAC implantation induced long-term LCAT activity in the patient with FLD, the stationary levels remained at approximately 5% of the value in a healthy person (392 ± 34.1 mU/mL). Despite the induction of LCAT activity by the LCAT-GMAC implantation, no alteration was seen in the levels of LCAT protein as determined by ELISA, presumably because of the low level of induction of LCAT protein (Table 6). The LCAT-GMAC implantation did not result in the development of autoantibodies against LCAT (Table 6).

3.4. Changes in serum lipid level, lipoprotein-cholesterol level, and lipoprotein profile

The serum TC level of the patient was markedly low, but his serum triglyceride (TG) level was within the normal range at the time of eligibility examination. The serum TG level of the patient was within the normal range (less than 150 mg/mL, Figure 5B and Table 6), except for the fourth and seventh days after implantation when the levels were higher than the normal range (175 mg/dL and 158 mg/dL, respectively). In contrast, the serum TC level of the patient was almost unchanged; it remained below the normal range (49–94 mg/dL) throughout the study period (Figure 5B and Table 6). At the time of eligibility assessment, the patient exhibited severely low serum LDL-C and HDL-C levels. Despite the induction of serum LCAT activity, the HDL-C level was almost unchanged after LCAT-GMAC implantation (Figure 5C and Table 6). In contrast, LDL-C level decreased slightly after implantation, bottomed 16

Table 11. Height, weight and vital signs.

Date		Days	Weeks	Height (cm)	Weight (kg)	Body Temperature (°C)	Pulse rate (BPM)	Systolic blood pressure (mmHg)	Diastolic blood pressure (mmHg)
2017	1/25	−29		173.3	56.3	36.4	77	135	79
	2/2	−21		172.9	56.7	37.0	76	134	82
	2/22	−1		172.9	58.0	36.5	74	117	73
	2/24	1		172.9	57.8	36.6	78	107	71
	2/27	4		ND	57.6	36.4	68	117	72
	3/2	7	1	ND	ND	ND	ND	ND	ND
	3/9	14	2	ND	57.6	36.7	103	134	75
	3/22	27	4	173.4	57.6	36.5	65	124	77
	4/6	42	6	173.4	57.2	36.8	102	136	79
	4/20	56	8	ND	56.8	36.4	82	131	75
	5/1	67	10	ND	56.2	36.5	82	135	74
	5/18	84	12	172.9	56.0	36.8	80	123	70
	6/16	113	16	173.3	56.5	37.0	81	140	88
	7/12	139	20	173.0	56.0	36.8	83	137	86
	8/9	167	24	173.1	56.5	36.6	68	136	82
	11/1	251	36	173.0	53.8	36.7	65	130	73
2018	1/24	335	48	173.0	59.0	36.6	81	155	92
	4/24	425	60	173.3	56.9	36.5	79	158	97
	7/9	501	72	173.4	55.7	36.7	88	150	99
	10/1	585	84	172.8	55.0	36.9	83	157	106
	12/27	672	96	173.0	56.1	36.0	98	117	64
2019	3/11	746	108	173.2	55.6	36.3	86	118	71
	6/3	830	120	173.2	54.8	36.9	102	112	74
	9/2	921	132	173.2	54.2	35.9	74	112	65
	11/27	1007	144	172.9	53.5	36.6	80	121	74
2020	2/17	1089	156	173.2	59.7	36.2	68	133	73
	5/11	1173	168	173.2	58.6	36.9	68	120	77
	8/17	1271	180	172.4	56.7	36.5	74	105	65
	10/28	1343	192	173.2	58.1	37.1	67	111	70
2021	1/18	1425	204	172.5	58.2	36.5	64	141	87
	4/12	1509	216	172.7	58.8	35.9	78	117	68
	7/12	1600	228	172.6	58.4	36.5	76	110	65
	10/6	1686	240	173.5	55.2	36.3	75	109	70

ND: not determined.

weeks after implantation, and gradually increased to pre-implantation levels 60 weeks after the implantation (Figure 5C and Table 6).

Consistent with the induction of LCAT activity, the free cholesterol (FC) level decreased rapidly after the implantation and lasted for more than two years except at 60 weeks; after 144 weeks of the implantation, it returned to the pre-implantation level (Figure 5D and Table 6). The LCAT-GMAC implantation rapidly increased the cholesterol ester (CE) level; after the temporal induction, it declined to below the basal levels by 60 weeks. After that, it increased modestly above the basal levels and was almost constant for over two years, except post-implantation weeks of 72 and 144 (Figure 5D, and Table 6). The %CE/TC showed a change comparable to that of the CE level (Figure 5D and Table 6). The patient's maximum %CE/TC increased to approximately 30%, which is still substantially lower than the normal range of 72%–77%.

The most noticeable change is a marked reduction in the level of intermediate-density lipoprotein (IDL), which is characteristic of FLD [33]. As revealed by polyacrylamide disc gel electrophoresis (PAGE) analysis, the IDL fraction gradually decreased over 24 weeks after implantation (Figure 5E). At 96 weeks after implantation, the lipoprotein pattern obtained by PAGE analysis was almost indistinguishable from the typical normal pattern. Based on its strong association with FLD [33], the reduction of IDL by the LCAT-GMAC may reflect the decrease of LP-X, an atypical vesicle in FLD, and is widely believed to be at least partially responsible for the progression of renal disease due to its unesterified cholesterol content [8, 34].

Gel permeation-HPLC (GP-HPLC) analysis revealed a remarkable alteration of lipoprotein profiles. The most noticeable change was TG reduction in VLDL fractions by the LCAT-GMAC implantation, as shown in Figure 6A and Table 7. In contrast, CE, FC, and phospholipid distribution in all lipoprotein fractions were almost unaltered. Furthermore, FC levels in the very small and the small HDL fractions were markedly reduced by the LCAT-GMAC implantation (Figure 6B). No apparent alteration was seen in fraction eight (lp8), previously shown to be associated with FLD [35]. The discrepancy between the results obtained using PAGE and HPLC analyses is due to detecting lipids. In PAGE analysis, Sudan Black B was used to stain lipids including cholesterol, TG, and phospholipid [24], whereas HPLC analysis utilizes enzymatic determination of cholesterol and TG [26, 36].

The plasma levels of major apolipoproteins are shown in Table 6. Along with HDL-C level, plasma ApoA-I level was almost unchanged by the implantation. In contrast, ApoB level increased immediately after the implantation, peaked four to seven days after implantation, decreased gradually by post-implantation week 4, and remained constant. ApoE level was almost unchanged before and after LCAT-GMAC implantation.

3.5. Hemolytic anemia

The patient had mild anemia when he was diagnosed at the age of 30 (blood hemoglobin level = 11.3 g/dL; grade I). His blood hemoglobin level remained in the range of mild anemia from the eligibility

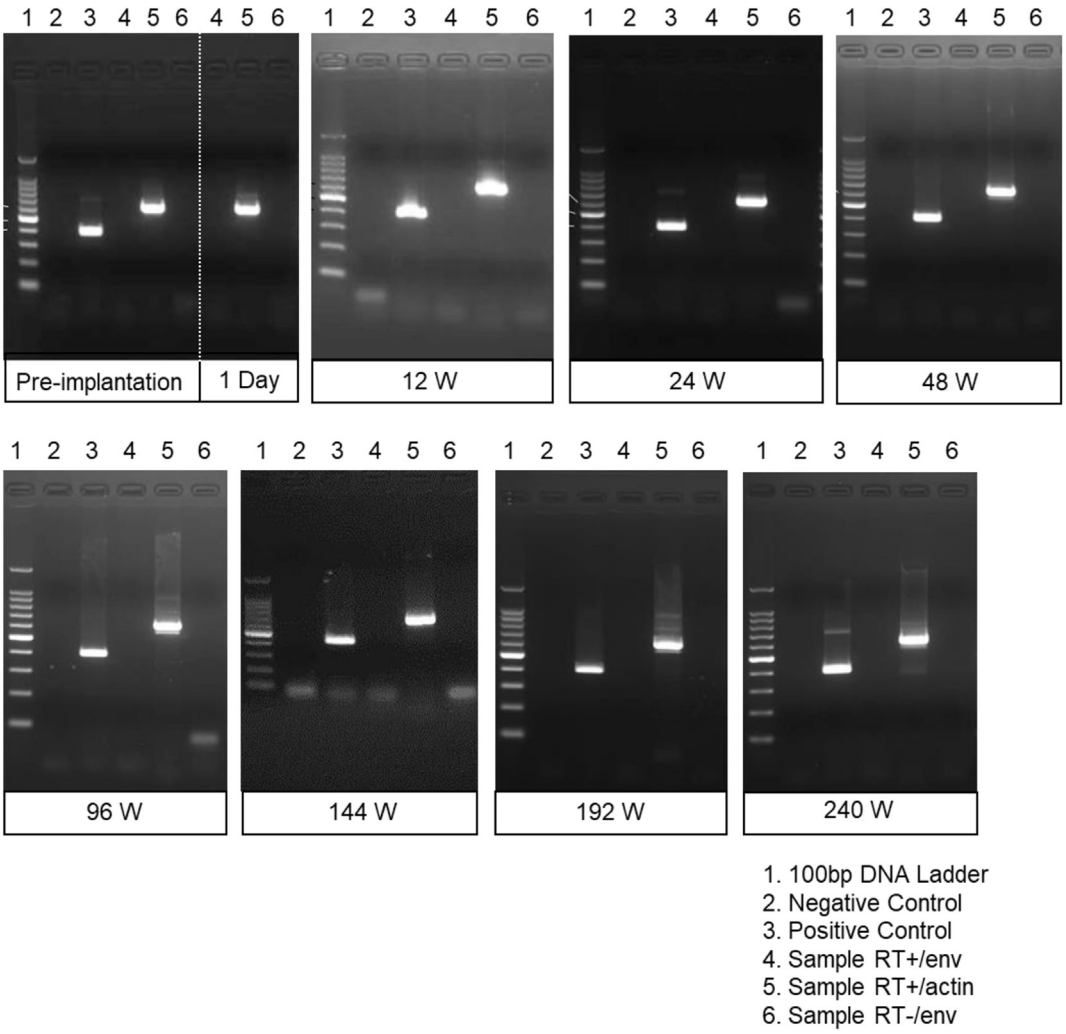

Figure 3. RCR test.
Blood samples taken from the patient implanted with LCAT-GMACs were tested for the presence of RCR using PCR amplification with *env*-specific primers. Total RNA from 400 μL of blood samples at the indicated time point was reverse-transcribed (50 ng) and subjected to PCR. The negative control contained no RNA, and the positive control contained 50 ng total RNA from SupT1 cells mixed with *env*-expressing GP + env-AM12 cells (10^5:1). PCR amplifications were performed using *env*-specific primers (labeled, env) or human actin-specific primers (labeled, actin). Gels were stained with ethidium bromide. Uncropped original image of 3 is shown as supplementary material (S).

assessment to 240 weeks after implantation (Figure 7A and Table 5). Further, his serum lactate dehydrogenase (LDH) level, one of the blood markers of anemia, was slightly higher than the upper limit of the normal range (266 U/L; normal range: 135–235 U/L) at the eligibility assessment. From immediately before the implantation to four weeks after the implantation, his LDH level fluctuated around 200 U/L (Figure 7A and Table 5). However, beyond four weeks after the implantation, his LDH level stabilized below 200 U/L, except at 84 weeks after implantation (Figure 7A and Table 5). The hematocrit, mean corpuscular volume (MCV), and mean corpuscular hemoglobin concentration (MCHC), which are indicators of anemia, were almost constant within the normal range (Table 8).

Despite the almost normal MCV and MCHV, visual inspection of the patient's serum revealed apparent hemolysis before the implantation (day −29, day −21) and post-implantation days 4, 7, and 27 [indicated by the red asterisk in the lower portion of Figure 7A and (1+) in Table 8). After four weeks following implantation, no visually detectable hemolysis was observed over three years.

We carried out a native-PAGE analysis to distinguish hemolysis that occurred *in vivo* or artificially occurred *in vitro* by blood sampling. By native-PAGE analysis, a 242-kDa protein was detected visually without staining (Figure 7B). This 242-kDa chromoprotein was detected mainly in hemolyzed samples but not in serum 20 weeks after the implantation (Figure 7B). A nano-LC/MS/MS analysis of the 242-kDa protein revealed that it consists of α and β chains of hemoglobin and haptoglobin. Hemoglobin released *in vitro* by freezing and thawing in healthy donor blood migrated for approximately 146-kDa (Figure 7C). Immunoblotting of the patient's serum using anti-human hemoglobin revealed an additional 200-kDa protein (Figure 7C).

We also analyzed sera from healthy volunteers that were hemolyzed due to improper blood draw technique. As shown in Figure 7D, two of the hemolyzed sera contained low levels of the 242-kDa protein (V2 and V3) detected by immunoblotting with anti-hemoglobin antibodies. The serum of volunteer 2 contained markedly high levels of free hemoglobin (146-kDa, Figure 7D). In hemolyzed sera from healthy volunteers, most hemoglobin proteins migrate as high molecular weight heterogeneous polymers, whereas no bands were detectable in pooled serum of healthy donors (Figure 7D). Immunoblotting with anti-haptoglobin antibodies revealed a 242-kDa band in volunteer 2 and a 200-kDa band in addition to a 242-kDa band in volunteer 3 (Figure 7E). Immunoblotting with anti-haptoglobin antibodies (Figure 7E) showed most haptoglobin proteins in healthy donors migrate as high molecular polymers. The presence of

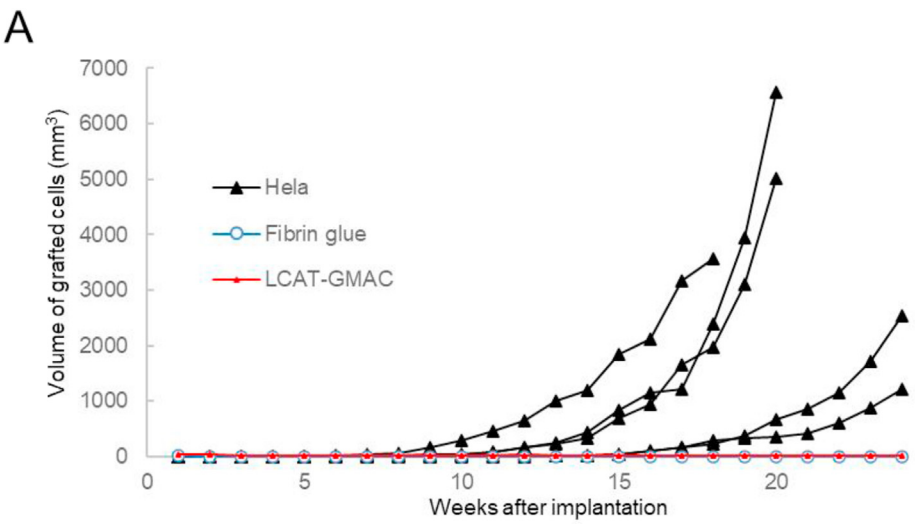

Weeks		1	2	3	4	5	6	7	8	9	10	11	12	13	14	15	16	17	18	19	20	21	22	23	24
HeLa	Mean	0	0	0	0	0	2	2	2	5	10	12	28	25	31	49	105	173	273	362	519	647	882	1308	1882
	SD	0	0	0	0	1	4	7	11	30	54	85	115	183	214	331	377	555	638	89	136	173	233	347	507
Fibrin glue	Mean	22	0	0	0	0	0	0	0	0	0	0	0	0	0	0	0	0	0	0	0	0	0	0	0
	SD	41	0	0	0	0	0	0	0	0	0	0	0	0	0	0	0	0	0	0	0	0	0	0	0
LCAT-GMAC	Mean	39	35	19	19	25	35	28	23	27	24	27	22	20	15	23	20	27	28	23	23	24	29	22	33
	SD	30	17	13	10	14	27	17	20	29	26	23	20	15	10	18	13	23	20	21	15	13	25	11	17

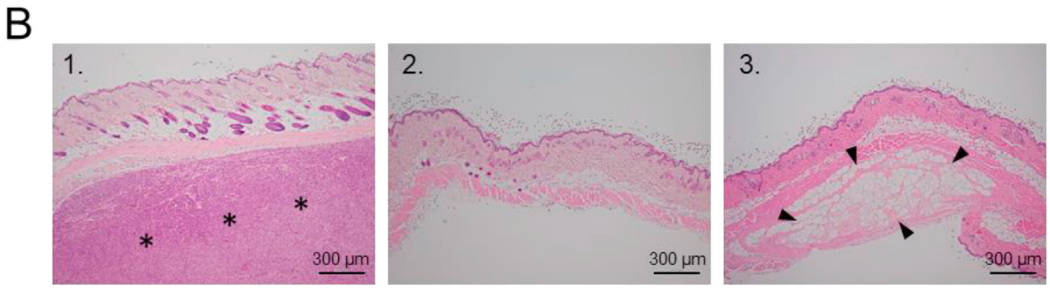

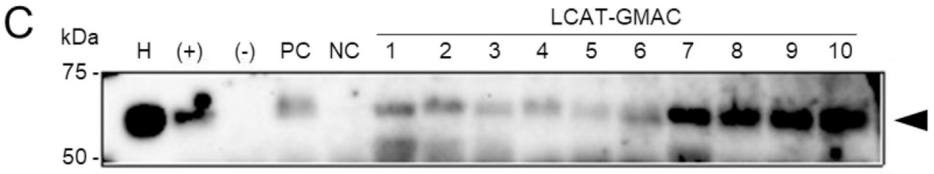

Figure 4. ***In vivo*** **tumorigenicity tests for LCAT-GMAC derived from the patient and control HeLa cells.**
Panel A. Graft cell volumes of NSG mice implanted with LCAT-GMACs or HeLa cells. LCAT-GMACs (1×10^7 cells/mouse, n = 10) or HeLa cells (1×10^5 cells/mouse, n = 5) were injected subcutaneously into NSG mice as described in Methods. The graft cell volumes of individual mice are shown in the upper panel. The mean graft cell volumes are shown in the lower panel. Due to overgrowth of the HeLa cells, one mouse was sacrificed 18 weeks after implantation, and two mice were sacrificed 20 weeks after implantation. The graft cell volumes of LCAT-GMACs implanted into the mice were unchanged, whereas HeLa cells developed a palpable mass by eight weeks after implantation. No graft cell volume was detected in mice injected with the cell suspension solution without cells (labeled Fibrin glue). Panel B. Histological findings in subcutaneous engraft of HeLa cells (the left image), cell suspension solution without cells (the middle image), and LCAT-GMACs from the patient (the right image). Representative images of histological analysis (hematoxylin and eosin staining) are shown. In NSG mice injected with HeLa cells, a robust outgrowth of the tumor was detected (indicated by asterisks). In contrast, no tumor was observed in mice injected with the cell suspension solution without cells (the middle image) or LCAT-GMACs (the right image). Note the fat cell accumulation in mice injected with LCAT-GMACs (indicated by arrow heads). Panel C. Western Blot Analysis of Immunoprecipitation (IP-Western) of sera of mice injected with LCAT-GMACs. Lane H denotes 1 μg of HDL; lane (+), 1 μg of HDL processed for immunoprecipitation; lane (−), none; lane PC, serum from HeLa cell injected mouse; lane NC, serum from a mouse injected the cell suspension solution without cells, lanes 1–10, serum from individual mouse implanted LCAT-GMACs. 100 μL serum samples (except for lane 2, 85μL) were immunoprecipitated and subjected to immunoblotting. The 60-kDa band detected in lane PC represents HeLa cell-derived LCAT protein, as revealed by IP western of the culture medium of HeLa cells. Uncropped original image of C is shown as supplementary material (S).

haptoglobin polymers is discussed below. Based on the results with the hemolyzed sera of healthy volunteers, the hemoglobin/haptoglobin complex in FLD patients was not caused by blood sampling.

Next, we analyzed the presence of the hemoglobin/haptoglobin complex using native-PAGE and subsequent immunoblotting. The 200-kDa and 242-kDa bands recognized by anti-hemoglobin antibodies

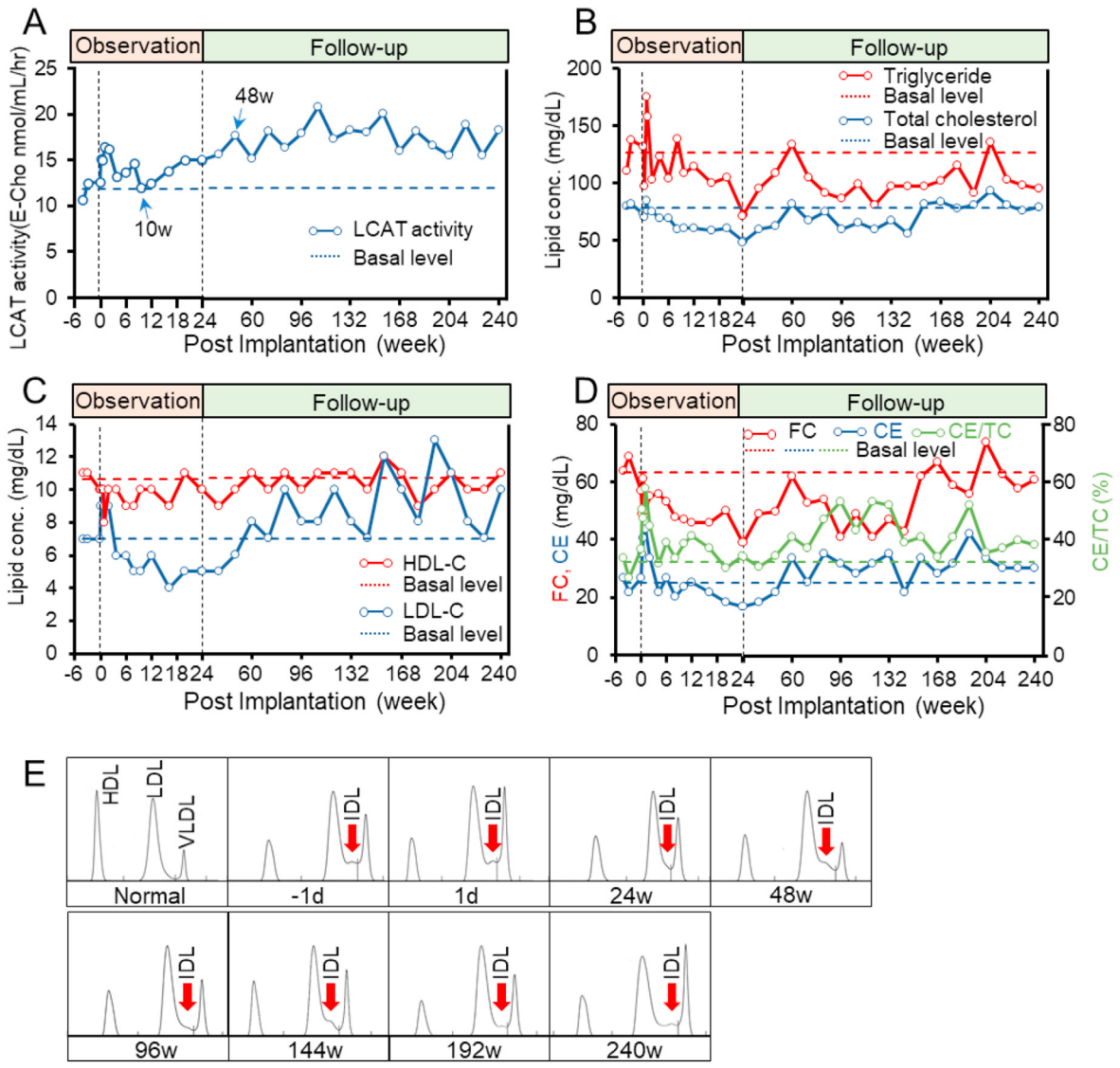

Figure 5. Changes in serum LCAT activity, serum lipids and lipoproteins.
(A). Changes in serum LCAT activity before and after LCAT-GMAC implantation. Arrows labeled 10w, and 48w indicate the post-implantation 10 weeks and 48 weeks, respectively. (B). Serum levels of TG and TC. (C). Serum HDL-cholesterol and LDL-cholesterol levels. (D). Changes in serum free cholesterol (FC), cholesteryl ester (CE) level and %cholesteryl ester/cholesterol before and after the implantation. CE concentration was calculated according to Okazaki and Yamashita [26]: 1.684 × (TC-FC) in mg/dL. The dashed line indicates the basal level. (E). Polyacrylamide gel disc electrophoresis of serum lipoproteins. Electrophoretic separation of lipoprotein fractions was performed according to the procedure as described [24]. Bold arrows indicate IDL fractions.

appeared on pre-implantation days -29, -21, and -1, and post-implantation days 1, 4, and 7 (Figure 7F). Except for post-implantation weeks 20, 48, and 84, the 200-kDa and 242-kDa bands were barely detectable after seven days following implantation. With the anti-hemoglobin antibodies, no signal was detected in the pooled sera from healthy donors. A similar result was obtained with anti-haptoglobin antibodies (Figure 7G). In healthy donors, most of the hemoglobin and haptoglobin proteins migrate as high molecular heterogeneous polymers. In contrast, only two forms of hemoglobin/haptoglobin complex were found in the patient. This difference may relate to the significantly lowered apoA1 level in the patient; apoA1-containing HDL is shown to be associated with haptoglobin and hemoglobin [37, 38]. There was no apparent relationship between serum haptoglobin level and the hemoglobin/haptoglobin complex (Table 5). These data suggest that the hemoglobin/haptoglobin complex was generated by intravascular hemolysis. LCAT-GMAC implantation may prevent the formation of hemoglobin/haptoglobin complex, thereby improving hemolysis.

3.6. Renal parameters, proteinuria, and blood pressure

In the whole course of the study, the patient had a clinically normal range of renal parameters, including serum creatinine level and cystatin C-based estimated glomerular filtration rate (Figure 8A and Table 5). Despite the almost normal renal parameters, the patient had proteinuria at the time of eligibility assessment. Immediately after the LCAT-GMAC implantation, the 24-hour urinary protein rapidly dropped to mild proteinuria (390 mg/d, Figure 8B and Tables 9 and 10, category A2, ≥150 mg/day and <500 mg/day) from severe proteinuria (category A3, ≥500 mg/day). After four weeks following the implantation, the proteinuria level gradually increased without deterioration of renal parameters and peaked at post-implantation week 60 (Figure 8B and Table 10). Consistent with the increased proteinuria, hyaline and epithelial casts were detected in urinary sediments at 12 weeks and 24 weeks after implantation (Table 9). Furthermore, dozens of red blood cells were detected in urinary sediments at post-implantation weeks 6, 8, 10, 16, 24, 60, and 84 (Table 9). The increased proteinuria level and the presence of epithelial

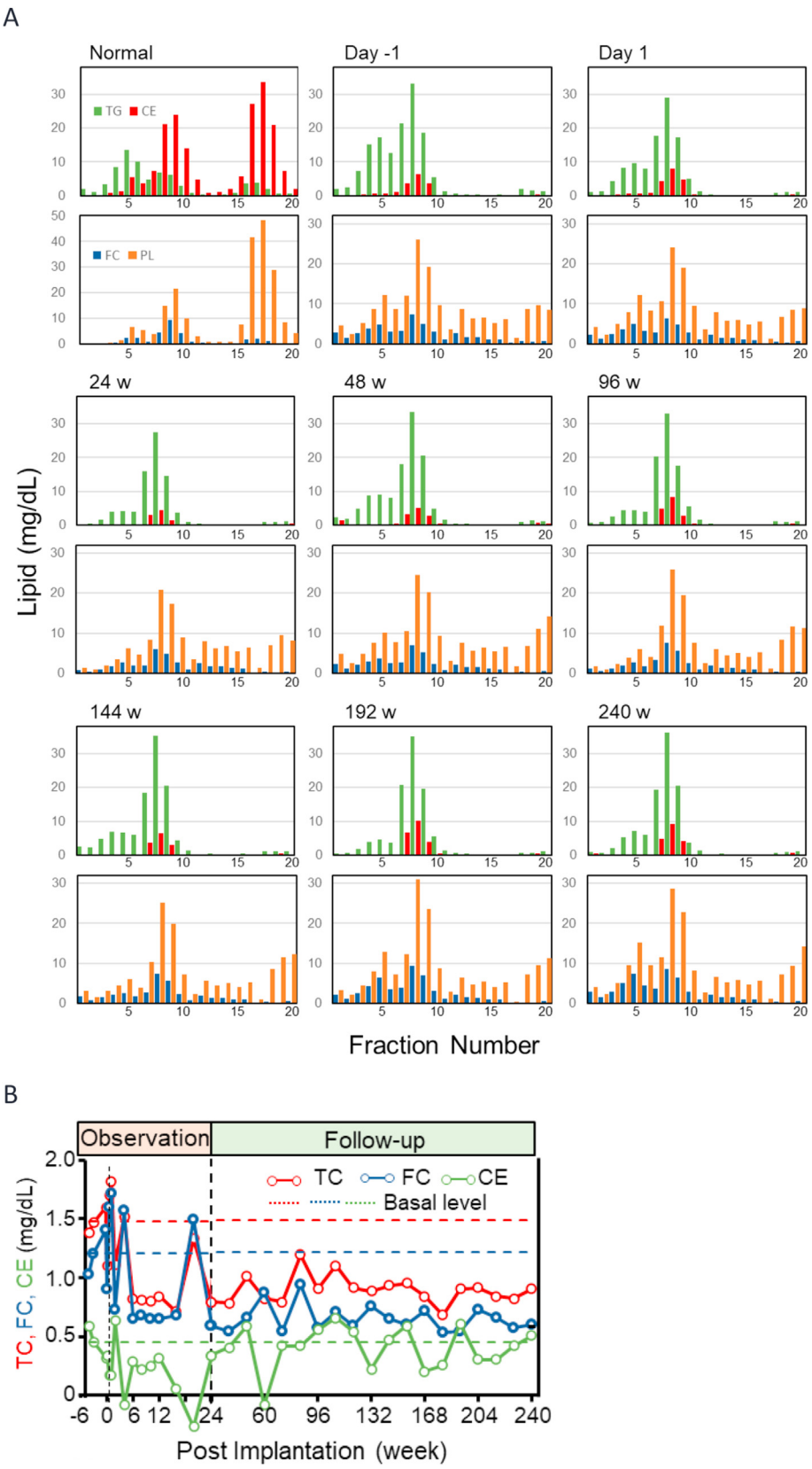

Figure 6. Changes in lipids in subclasses of lipoprotein separated by gel permeation-HPLC (GP-HPLC).

(A). TG, CE, FC, and phospholipid (PL) levels in the 20 subfractions of lipoprotein separated by GP-HPLC are shown. Representative data in pre (−1) and-post-LCAT-GMAC implantation (+1 day, and 24–240 weeks) are shown. The values in all the time points are shown in Table 7. CE concentration was calculated according to Okazaki and Yamashita [26]. (B). Changes in TC, FC, and CE levels of the small HDL (subfraction 18) and very small HDL (subfraction 19) determined by GP-HPLC are shown. (C), Values of TC, FC, and CE contents are shown in the small HDL (subfraction 18) and very small HDL (subfraction 19) separated by GP-HPLC at the indicated time point.

casts and red blood cells in urinary sediments may be due to the progression of renal injury.

After 48 weeks of implantation, the patient developed mild hypertension (Figure 8C and Table 10). At post-implantation week 72, the patient started treatment of telmisartan, an angiotensin-receptor blocker (ARB). However, Telmisartan did not improve hypertension (Figure 8C and Table 11). Micamlo, a combination tablet of telmisartan and the calcium-channel blocker amlodipine, was then administered to the

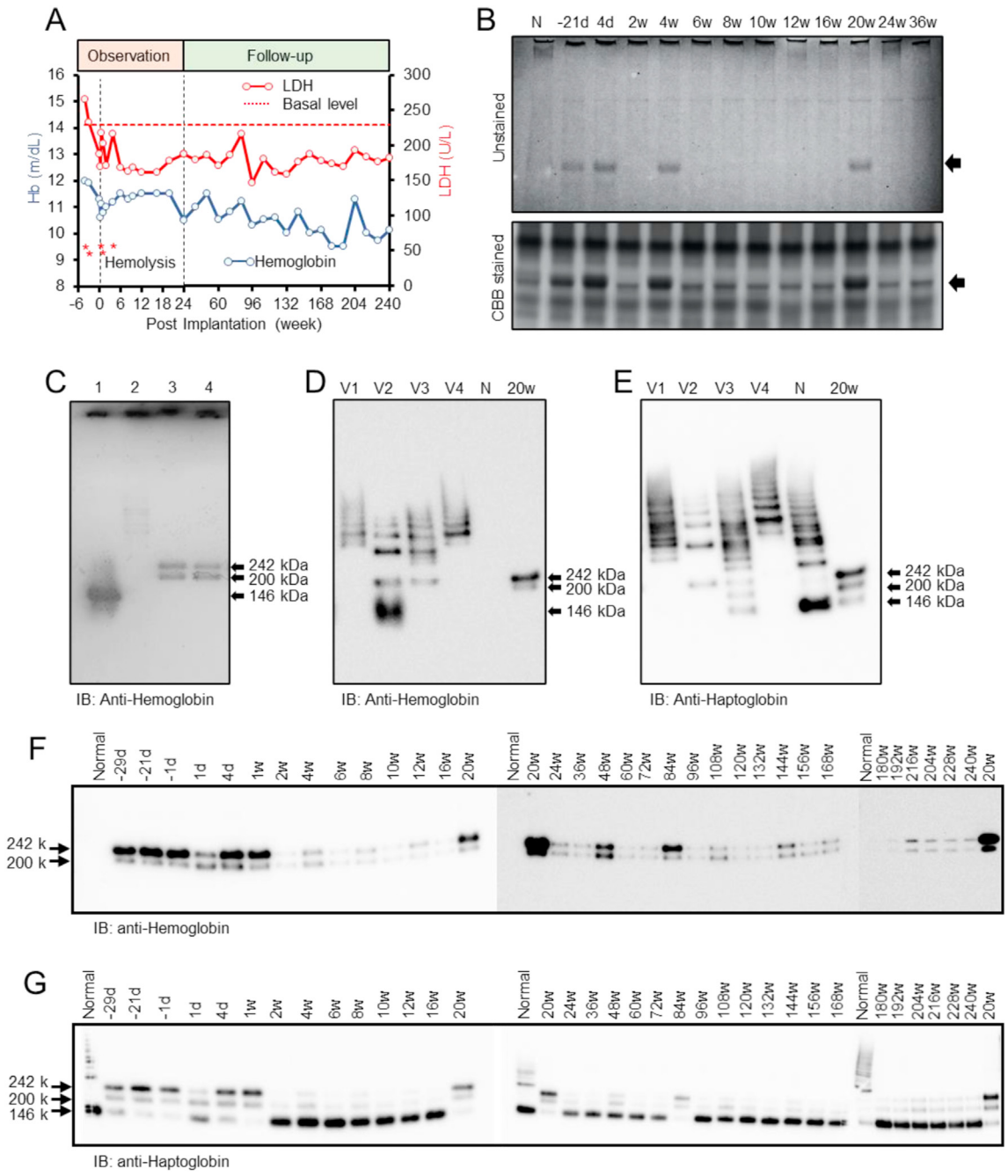

Figure 7. Biochemical parameters of anemia and presence of hemoglobin/haptoglobin complex.
(A). Serum levels of hemoglobin and lactate dehydrogenase (LDH) before and after implantation. Visually detectable hemolysis is indicated by red asterisks. The dashed line indicates the basal level. (B). Native polyacrylamide gel electrophoresis of serum proteins before and after implantation. The upper panel shows the gel without staining, and the lower panel shows the same gel stained with Coomassie Brilliant Blue G-250. As described in Methods, 7 μL of serum at the indicated time points were electrophoresed. Arrows indicate the 242-kDa chromoprotein detected without protein staining. (C). Immunoblot analysis of frozen and thawed blood (0.01 μL) from a healthy donor (lane 1). Pooled serum of healthy donors (0.1 μL, lane 2) and the patient's serum at pre-implantation day −21 (0.1 μL, lane 3) and post-implantation day 1 (0.1 μL, lane 4) were subjected to electrophoresis and subsequent immunoblotting (IB) using anti-human hemoglobin antibodies. (D, E). Immunoblotting of hemolyzed sera from healthy volunteers. Hemolyzed sera (0.1 μL) from healthy volunteers (V1–V4), pooled serum of healthy donors (0.1 μL, N) and the patient's serum at post-implantation week 20 (0.1 μL, 20w) were electrophoresed and subjected to immunoblotting with anti-human hemoglobin (D) or with anti-human haptoglobin antibodies (E). (F, G). Immunoblot analysis of patient's serum proteins before and after implantation. The patient's serum (0.1 μL) indicated time points were electrophoresed and analyzed using immunoblotting with anti-hemoglobin (F) or with anti-human haptoglobin antibodies (G). Uncropped original images of (B–G) are shown as supplementary materials (BS–GS).

patient at 84 weeks of implantation. This treatment resulted in the normalization of his blood pressure (Figure 8C and Table 11).

With the normalization of his blood pressure, the 24-hour urine protein level rapidly dropped to mild proteinuria from severe proteinuria. Similarly, urinary β2-microglobulin level fell to normal range after 96 weeks following post-implantation. The reduced proteinuria lasted over two years after the 96 weeks of the implantation (Figure 8B and Table 10).

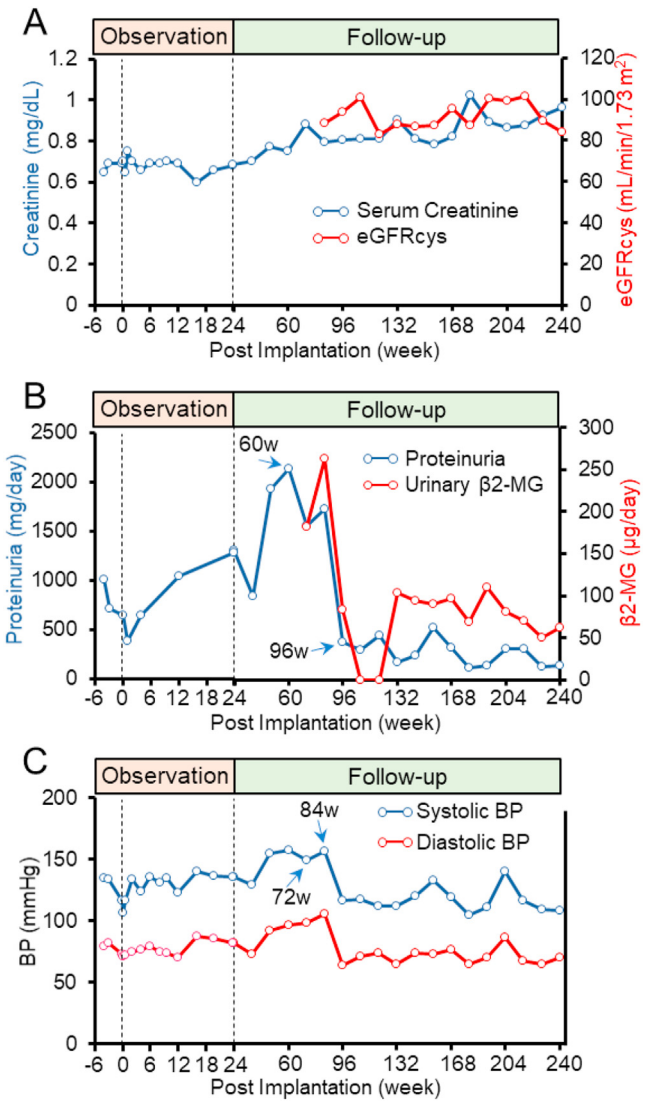

Figure 8. Renal parameters, proteinuria, and blood pressure.
(A) Serum levels of creatinine and cystatin-C-based estimates of glomerular filtration rate (eGFRcys) before and after implantation are shown. (B) 24-hour urinary protein and β2-microglobulin levels before and after implantation. Arrows labeled 60w, and 96w indicate the time points the post-implantation 60 weeks and 96 weeks, respectively. (C) Changes in blood pressure. Arrows labeled 72, and 84 indicate the time points when ARB and ARB plus calcium-channel blockers were administered to the patient.

4. Discussion

This study first showed that LCAT-GMAC implantation, an *ex vivo* gene therapy, is a safe and effective treatment for FLD. The most notable finding is that LCAT-GMAC implantation ameliorates hemolysis and proteinuria in a patient with FLD.

Although LCAT-GMAC implantation induced long-term LCAT activity, the stationary level remained at approximately 5% of the level in a healthy person (Figure 5A and Table 6). This level of LCAT activity may be sufficient for improving the lipoprotein profile, anemia, and proteinuria. However, it was not enough to improve the HDL-C level and corneal opacity; the patient did not show apparent improvement of corneal opacity. Immediately after the implantation, LCAT activity increased and sustained for two weeks (Figure 5A and Table 6). After that, it started to decrease and fell to the pre-implantation level by post-implantation week 10, and slowly recovered and almost plateaued 48 weeks after implantation (Figure 5A and Table 6). This decline in LCAT activity may be due to ischemic injury of the implanted cells. It is believed that ischemic injury of adipocytes occurs from implantation until revascularization occurs [39]. A similar post-implantation reduction in LCAT activity was observed in mice injected with syngeneic LCAT-GMACs [11]. The recovery of LCAT activity 24 weeks after implantation may be due to revascularization or remodeling of the blood vessels. Further improvement of LCAT-GMACs by enhancing LCAT copy numbers by using a highly efficient transduction vector, dose escalation of LCAT-GMACs, the introduction of an activated form of LCAT, or improved implantation methods may result in a complete form reversal FLD.

Despite the modest induction of LCAT activity by the LCAT-GMAC implantation, a marked reduction of IDL fraction was seen in PAGE analysis (Figure 5E). Based on the association IDL with FLD [33], the decrease of IDL by the LCAT-GMAC may reflect the decrease of LP-X, an atypical vesicle in FLD, and is widely believed to be at least partially responsible for the progression of renal disease due to its unesterified cholesterol content [8, 34]. Furthermore, GP-HPLC showed a noticeable reduction of TG in the VLDL fraction by the LCAT-GMAC implantation (Figure 6A and Table 7). The decrease of FC in the very small and the small fraction is noteworthy because these lipoproteins are the substrates for LCAT *in vivo* (Figure 6B and Table 7). The reduction of FC in the very small HDL and the small HDL fractions may result in decreased hemolysis and an improved lipoprotein profile.

Anemia in FLD is believed to be triggered by erythrocyte membrane vulnerability due to LCAT deficiency. The phospholipid composition of the erythrocyte membrane was markedly altered in an FLD patient [40]. This alteration may relate to the shape and the osmotic fragility of the erythrocytes. Our current data suggested that the LCAT-GMAC implantation improved erythrocyte vulnerability. The erythrocyte vulnerability may cause the occurrence of hemoglobin/haptoglobin complex (Figure 7 panels F and G).

The renal injury in FLD is believed to be caused by the deposition of excess lipid in the glomerulus, mesangial cells, and renal tubules, as revealed by electron microscopy [41]. The renal deposition of lipids may be caused by impaired reverse cholesterol transportation due to defective LCAT activity. According to Samburek et al., enzyme replacement therapy with recombinant LCAT for a patient with FLD appeared to improve proteinuria, stabilize renal function, and delay imminent dialysis by eight months [10]. In this study, a rapid decrease in proteinuria level was observed immediately after the implantation (Figure 8B and Table 10). After the rapid reduction of proteinuria, it was worse afterward, accompanied by the declined LCAT activities (post-implantation weeks 4–36) (Figures 5A and 8B, and Tables 6 and 10). This reduction may affect the deterioration of renal function.

The reduction in proteinuria level occurred almost simultaneously with the decrease in blood pressure following an ARB and a calcium-channel blocker administration (Figures 8B and 8C, and Tables 10 and 11). Renin-angiotensin system (RAS) inhibitors, commonly used antihypertensive drugs, exhibit renoprotective effects, thereby reducing proteinuria [42]. Combined treatment with calcium-channel blockers with RAS inhibitors showed no additive renoprotective effects than RAS inhibitors only [43]. In this study, ARB alone did not reduce blood pressure and proteinuria (Figures 8B and 8C, and Tables 10 and 11). Therefore, the effects of combining an ARB and a calcium-channel blocker on rapidly reducing proteinuria from 96 weeks of the implantation remains unclear. Under the normotensive, immediately after the implantation, the proteinuria was temporarily reduced to mild levels (Figures 8B and 8C, and Tables 10 and 11). ARB is shown to have potent proteinuria reducing effect in addition to the reduction of blood pressure. Either treatment with telmisartan or valsartan for 12 months reduced the urinary protein excretion rate (24 h) by approximately 35% from the baselines in hypertensive patients with type 2 diabetes mellitus and overt nephropathy [44]. In a case of an FLD patient, losartan treatment combined with a fat restriction reduced proteinuria by 70% after one year of therapy [45]. In this case, the level of proteinuria remained within the overt proteinuria. Given the limited effect of ARBs on proteinuria, the

anti-hypertensives alone cannot account for the urinary protein reduction in the patient. GMAC mediated supplementation of LCAT appears to play a part in reducing proteinuria.

Various epidemiological studies showed that not all FLD patients cause kidney injury. Despite a complete lack of LCAT activity, some patients do not develop hemolytic anemia or renal disease. In Brazilian cases of FLD, anemia was observed in 25 out of 38 patients, in almost all patients with renal insufficiency [2]. A comprehensive and systematic review of the LCAT deficiency showed that about 50% of patients develop renal injuries [46]. LP-X is suggested to be the leading cause of renal injury [8], but the exact cause of renal dysfunction in FLD is unknown. Although the development of renal injury remains unclarified, a modest supplementation of functional LCAT may lead to the improvement of renal injury by reducing LP-X. Alternatively, other susceptible factors may be associated with anemia and renal injury. A modest supplementation of functional LCAT may reduce such susceptible factors. Further studies are required to elucidate the exact role of LCAT in the pathogenesis of renal injury.

In conclusion, our current data suggest that GMAC-mediated therapy appears to be a safe, long-lasting, and promising treatment option for intractable genetic diseases.

4.1. Limitation of study

Due to the extremely low genetic prevalence of FLD (less than one in a million), there was a limitation in recruiting patients eligible for this clinical study. Only a young male carrying missense mutation at proline 69 replaced with leucine willingly participated in this study. There are no common mutations found in FLD. Therefore, the results obtained using only one patient with a particular mutation cannot apply to other FLD patients without limitations. There may be a genetic and environmental background that may affect the efficiency of LCAT-GMAC implantation.

Declarations

Author contribution statement

Masayuki Aso, Koutaro Yokote and Yasushi Saito: Conceived and designed the experiments; Analyzed and interpreted the data; Wrote the paper.

Tokuo T. Yamamoto: Conceived and designed the experiments; Performed the experiments; Analyzed and interpreted the data; Wrote the paper.

Masayuki Kuroda, Hideki Hanaoka: Conceived and designed the experiments; Analyzed and interpreted the data.

Jun Wada, Yasuyuki Aoyag: Performed the experiments; Analyzed and interpreted the data; Contributed reagents, materials, analysis tools or data.

Yoshitaka Kubota, Akinobu Onitake, Yuta Matsuura, Shun-ichi Konno, Katsuaki Nishino, Masami Tanio, Takayuki Ikeuchi, Nobuyuki Mitsukawa: Performed the experiments; Contributed reagents, materials, analysis tools or data.

Ko Ishikawa, Yoshiro Maezawa, Naoya Teramoto, Ayako Tawada, Sakiyo Asada: Performed the experiments; Analyzed and interpreted the data.

Mika Kirinashizawa, Misato Yamamoto, Junko Miyoshi, Hidetoshi Igari: Performed the experiments.

Kunio Yasunaga: Analyzed and interpreted the data; Wrote the paper.

Norihiko Kobayashi, Hidetoshi Igar, Yasushi Saito: Analyzed and interpreted the data.

Funding statement

Dr. Tokuo Yamamoto was supported by Setsuro Fujii Memorial The Osaka Foundation for Promotion of Fundamental Medical Research [J17KF00092].

Masayuki Aso was supported by Japan Agency for Medical Research and Development [JP 17im0110606h0004].

Data availability statement

Data included in article/supplementary material/referenced in article.

Declaration of interest's statement

The authors declare the following conflict of interests:

Tokuo Yamamoto is an employee of CellGenTech, Inc. and Chiba University during the study. Masayuki Kuroda reports Joint research funds from CellGenTech, Inc. during the study. The other authors have nothing to disclose.

Additional information

Supplementary content related to this article has been published online at https://doi.org/10.1016/j.heliyon.2022.e11271.

Acknowledgements

We thank the participant for his altruism and his dedication to this study; the donors who provided adipocytes for their contribution to the development of LCAT-GMAC; the members of the Chiba University Clinical Research Center for their help in clinical data management and safety monitoring; and the members of CellGenTech, inc., for the preparation and quality control analysis of LCAT-GMAC. Special thanks to Dr. Mitsuyo Okazaki (Tokyo Medical and Dental University) for her excellent assistance, advice, and discussion on lipoprotein analysis.

References

[1] S. Santamarina-Fojo, J.M. Hoeg, G. Assmann, J.H. Bryan Brewer, Lecithin cholesterol acyltransferase deficiency and fish eye disease, in: D.L. Valle, S. Antonarakis, A. Ballabio, A.L. Beaudet, G.A. Mitchell (Eds.), The Online Metabolic and Molecular Bases of Inherited Disease, McGraw-Hill, New York, 2001.

[2] K.R. Norum, A.T. Remaley, H.E. Miettinen, E.H. Strøm, B.E.P. Balbo, C. Sampaio, I. Wiig, J.A. Kuivenhoven, L. Calabresi, J.J. Tesmer, M. Zhou, D.S. Ng, B. Skeie, S.K. Karathanasis, K.A. Manthei, K. Retterstøl, Lecithin:cholesterol acyltransferase: symposium on 50 years of biomedical research from its discovery to latest findings, J. Lipid Res. 61 (2020) 1142–1149.

[3] S. Kunnen, M. Van Eck, Lecithin:cholesterol acyltransferase: old friend or foe in atherosclerosis? J. Lipid Res. 53 (2012) 1783–1799.

[4] C.C. Schwartz, J.M. VandenBroek, P.S. Cooper, Lipoprotein cholesteryl ester production, transfer, and output in vivo in humans, J. Lipid Res. 45 (2004) 1594–1607.

[5] J.A. Kuivenhoven, H. Pritchard, J. Hill, J. Frohlich, G. Assmann, J. Kastelein, The molecular pathology of lecithin:cholesterol acyltransferase (LCAT) deficiency syndromes, J. Lipid Res. 38 (1997) 191–205.

[6] A.S. Geller, E.Y. Polisecki, M.R. Diffenderfer, B.F. Asztalos, S.K. Karathanasis, R.A. Hegele, E.J. Schaefer, Genetic and secondary causes of severe HDL deficiency and cardiovascular disease, J. Lipid Res. 59 (2018) 2421–2435.

[7] R.M. Stoekenbroek, M.A. van den Bergh Weerman, G.K. Hovingh, B.J. Potter van Loon, C.E. Siegert, A.G. Holleboom, Familial LCAT deficiency: from renal replacement to enzyme replacement, Neth. J. Med. 71 (2013) 29–31.

[8] B.L. Vaisman, E.B. Neufeld, L.A. Freeman, S.M. Gordon, M.L. Sampson, M. Pryor, E. Hillman, M.J. Axley, S.K. Karathanasis, A.T. Remaley, LCAT enzyme replacement therapy reduces LpX and improves kidney function in a mouse model of familial LCAT deficiency, J. Pharmacol. Exp. Therapeut. 368 (2019) 423–434.

[9] L.A. Freeman, S.K. Karathanasis, A.T. Remaley, Novel lecithin: cholesterol acyltransferase-based therapeutic approaches, Curr. Opin. Lipidol. 31 (2020) 71–79.

[10] R.D. Shamburek, R. Bakker-Arkema, B.J. Auerbach, B.R. Krause, R. Homan, M.J. Amar, L.A. Freeman, A.T. Remaley, Familial lecithin:cholesterol acyltransferase deficiency: first-in-human treatment with enzyme replacement, J. Clin. Lipidol. 10 (2016) 356–367.

[11] Y. Aoyagi, M. Kuroda, S. Asada, H. Bujo, S. Tanaka, S. Konno, M. Tanio, I. Ishii, M. Aso, Y. Saito, Fibrin glue increases the cell survival and the transduced gene product secretion of the ceiling culture-derived adipocytes transplanted in mice, Exp. Mol. Med. 43 (2011) 161–167.

[12] S. Asada, M. Kuroda, Y. Aoyagi, H. Bujo, S. Tanaka, S. Konno, M. Tanio, I. Ishii, M. Aso, Y. Saito, Disturbed apolipoprotein A-I-containing lipoproteins in fish-eye disease are improved by the lecithin:cholesterol acyltransferase produced by gene-transduced adipocytes in vitro, Mol. Genet. Metabol. 102 (2011) 229–231.

[13] S. Asada, M. Kuroda, Y. Aoyagi, Y. Fukaya, S. Tanaka, S. Konno, M. Tanio, M. Aso, K. Satoh, Y. Okamoto, T. Nakayama, Y. Saito, H. Bujo, Ceiling culture-derived proliferative adipocytes retain high adipogenic potential suitable for use as a vehicle for gene transduction therapy, Am. J. Physiol. Cell Physiol. 301 (2011) C181–185.
[14] M. Kuroda, Y. Aoyagi, S. Asada, H. Bujo, S. Tanaka, T. Konno, M. Tanio, I. Ishii, K. Machida, F. Matsumoto, Ceiling culture-derived proliferative adipocytes are a possible delivery vehicle for enzyme replacement therapy in lecithin: cholesterol acyltransferase deficiency, Open Gene Ther. J. 4 (2011) 1–10.
[15] M. Kuroda, A.G. Holleboom, E.S. Stroes, S. Asada, Y. Aoyagi, K. Kamata, S. Yamashita, S. Ishibashi, Y. Saito, H. Bujo, Lipoprotein subfractions highly associated with renal damage in familial lecithin:cholesterol acyltransferase deficiency, Arterioscler. Thromb. Vasc. Biol. 34 (2014) 1756–1762.
[16] M. Ito, H. Bujo, K. Takahashi, T. Arai, I. Tanaka, Y. Saito, Implantation of primary cultured adipocytes that secrete insulin modifies blood glucose levels in diabetic mice, Diabetologia 48 (2005) 1614–1620.
[17] H. Sugihara, N. Yonemitsu, S. Miyabara, S. Toda, Proliferation of unilocular fat cells in the primary culture, J. Lipid Res. 28 (1987) 1038–1045.
[18] K.L. Spalding, E. Arner, P.O. Westermark, S. Bernard, B.A. Buchholz, O. Bergmann, L. Blomqvist, J. Hoffstedt, E. Näslund, T. Britton, H. Concha, M. Hassan, M. Rydén, J. Frisén, P. Arner, Dynamics of fat cell turnover in humans, Nature 453 (2008) 783–787.
[19] P. Cohen, B.M. Spiegelman, Cell biology of fat storage, Mol. Biol. Cell 27 (2016) 2523–2527.
[20] J.H. Stern, J.M. Rutkowski, P.E. Scherer, Adiponectin, leptin, and fatty acids in the maintenance of metabolic homeostasis through adipose tissue crosstalk, Cell Metabol. 23 (2016) 770–784.
[21] X. Zhang, F.D. Cruz, M. Terry, F. Remotti, I. Matushansky, Terminal differentiation and loss of tumorigenicity of human cancers via pluripotency-based reprogramming, Oncogene 32 (2013) 2249–2260, 2260.e2241-2221.
[22] R. Ishibashi, M. Takemoto, Y. Tsurutani, M. Kuroda, M. Ogawa, H. Wakabayashi, N. Uesugi, M. Nagata, N. Imai, A. Hattori, K. Sakamoto, T. Kitamoto, Y. Maezawa, I. Narita, S. Hiroi, A. Furuta, T. Miida, K. Yokote, Immune-mediated acquired lecithin-cholesterol acyltransferase deficiency: a case report and literature review, J Clin Lipidol 12 (2018), 888–897.e882.
[23] C.A. Wilson, T.H. Ng, A.E. Miller, Evaluation of recommendations for replication-competent retrovirus testing associated with use of retroviral vectors, Hum. Gene Ther. 8 (1997) 869–874.
[24] A. Yoshida, M. Kodama, H. Nomura, M. Naito, Classification of lipoprotein profile by polyacrylamide gel disc electrophoresis, Intern. Med. 42 (2003) 244–249.
[25] M. Okazaki, S. Usui, M. Nakamura, S. Yamashita, Evaluation of an HPLC method for LDL-cholesterol determination in patients with various lipoprotein abnormalities in comparison with beta-quantification, Clin. Chim. Acta 395 (2008) 62–67.
[26] M. Okazaki, S. Yamashita, Recent advances in analytical methods on lipoprotein subclasses: calculation of particle numbers from lipid levels by gel permeation HPLC using “spherical particle model”, J. Oleo Sci. 65 (2016) 265–282.
[27] S. Usui, Y. Hara, S. Hosaki, M. Okazaki, A new on-line dual enzymatic method for simultaneous quantification of cholesterol and triglycerides in lipoproteins by HPLC, J. Lipid Res. 43 (2002) 805–814.
[28] S. Yamashita, M. Okazaki, T. Okada, D. Masuda, K. Yokote, H. Arai, E. Araki, S. Ishibashi, Distinct differences in lipoprotein particle number evaluation between GP-HPLC and NMR: analysis in dyslipidemic patients administered a selective PPARα modulator, pemafibrate, J. Atherosclerosis Thromb. 28 (2021) 974–996.
[29] A. Katayama, J. Wada, H.U. Kataoka, H. Yamasaki, S. Teshigawara, T. Terami, K. Inoue, M. Kanzaki, K. Murakami, A. Nakatsuka, H. Sugiyama, N. Koide, H. Bujo, H. Makino, Two novel mutations of lecithin:cholesterol acyltransferase (LCAT) gene and the influence of APOE genotypes on clinical manifestations, NDT Plus 4 (2011) 299–302.
[30] R.E. Donahue, S.W. Kessler, D. Bodine, K. McDonagh, C. Dunbar, S. Goodman, B. Agricola, E. Byrne, M. Raffeld, R. Moen, et al., Helper virus induced T cell lymphoma in nonhuman primates after retroviral mediated gene transfer, J. Exp. Med. 176 (1992) 1125–1135.
[31] L. Sastry, K. Cornetta, Detection of replication competent retrovirus and lentivirus, Methods Mol. Biol. 506 (2009) 243–263.
[32] L.D. Shultz, F. Ishikawa, D.L. Greiner, Humanized mice in translational biomedical research, Nat. Rev. Immunol. 7 (2007) 118–130.
[33] S. Murano, K. Shirai, Y. Saito, S. Yoshida, Y. Ohta, H. Tsuchida, S. Yamamoto, G. Asano, C.H. Chen, J.J. Albers, Impaired intermediate-density lipoprotein triglyceride hydrolysis in familial lecithin:cholesterol acyltransferase (LCAT) deficiency, Scand. J. Clin. Lab. Invest. 47 (1987) 775–783.
[34] A. Ossoli, E.B. Neufeld, S.G. Thacker, B. Vaisman, M. Pryor, L.A. Freeman, C.A. Brantner, I. Baranova, N.O. Francone, S.J. Demosky Jr., C. Vitali, M. Locatelli, M. Abbate, C. Zoja, G. Franceschini, L. Calabresi, A.T. Remaley, Lipoprotein X causes renal disease in LCAT deficiency, PLoS One 11 (2016), e0150083.
[35] T. Watanabe, T. Nema, N. Hiruta, T. Murano, W.J. Schneider, H. Bujo, Lp8 is potentially associated with partial lecithin:cholesterol acyltransferase deficiency in a patient with primary biliary cirrhosis, J. Clin. Lipidol. 12 (2018) 1157–1163.
[36] T. Fujino, H. Asaba, M.J. Kang, Y. Ikeda, H. Sone, S. Takada, D.H. Kim, R.X. Ioka, M. Ono, H. Tomoyori, M. Okubo, T. Murase, A. Kamataki, J. Yamamoto, K. Magoori, S. Takahashi, Y. Miyamoto, H. Oishi, M. Nose, M. Okazaki, S. Usui, K. Imaizumi, M. Yanagisawa, J. Sakai, T.T. Yamamoto, Low-density lipoprotein receptor-related protein 5 (LRP5) is essential for normal cholesterol metabolism and glucose-induced insulin secretion, Proc. Natl. Acad. Sci. U. S. A. 100 (2003) 229–234.
[37] J. Watanabe, V. Grijalva, S. Hama, K. Barbour, F.G. Berger, M. Navab, A.M. Fogelman, S.T. Reddy, Hemoglobin and its scavenger protein haptoglobin associate with apoA-1-containing particles and influence the inflammatory properties and function of high density lipoprotein, J. Biol. Chem. 284 (2009) 18292–18301.
[38] X. Ji, Y. Feng, H. Tian, W. Meng, W. Wang, N. Liu, J. Zhang, L. Wang, J. Wang, H. Gao, The mechanism of proinflammatory HDL generation in sickle cell disease is linked to cell-free hemoglobin via haptoglobin, PLoS One 11 (2016), e0164264.
[39] L. Shih, M.J. Davis, S.J. Winocour, The science of fat grafting, Semin. Plast. Surg. 34 (2020) 5–10.
[40] T. Suda, A. Akamatsu, Y. Nakaya, Y. Masuda, J. Desaki, Alterations in erythrocyte membrane lipid and its fragility in a patient with familial lecithin:cholesterol acyltrasferase (LCAT) deficiency, J. Med. Invest. 49 (2002) 147–155.
[41] M.M. Althaf, H. Almana, A. Abdelfadiel, S.M. Amer, T.O. Al-Hussain, Familial lecithin-cholesterol acyltransferase (LCAT) deficiency; a differential of proteinuria, J. Nephropathol. 4 (2015) 25–28.
[42] R. Kunz, C. Friedrich, M. Wolbers, J.F. Mann, Meta-analysis: effect of monotherapy and combination therapy with inhibitors of the renin angiotensin system on proteinuria in renal disease, Ann. Intern. Med. 148 (2008) 30–48.
[43] R.S. Huang, Y.M. Cheng, X.X. Zeng, S. Kim, P. Fu, Renoprotective effect of the combination of renin-angiotensin system inhibitor and calcium channel blocker in patients with hypertension and chronic kidney disease, Chin. Med. J. 129 (2016) 562–569.
[44] J. Galle, E. Schwedhelm, S. Pinnetti, R.H. Böger, C. Wanner, Antiproteinuric effects of angiotensin receptor blockers: telmisartan versus valsartan in hypertensive patients with type 2 diabetes mellitus and overt nephropathy, Nephrol. Dial. Transplant. 23 (2008) 3174–3183.
[45] S. Naito, M. Kamata, M. Furuya, M. Hayashi, M. Kuroda, H. Bujo, K. Kamata, Amelioration of circulating lipoprotein profile and proteinuria in a patient with LCAT deficiency due to a novel mutation (Cys74Tyr) in the lid region of LCAT under a fat-restricted diet and ARB treatment, Atherosclerosis 228 (2013) 193–197.
[46] C. Vitali, A. Bajaj, C. Nguyen, J. Schnall, J. Chen, K. Stylianou, D.J. Rader, M. Cuchel, A systematic review of the natural history and biomarkers of primary Lecithin:Cholesterol Acyltransferase (LCAT) deficiency, J. Lipid Res. (2022), 100169.